University of South Bohemia in České Budějovice

Faculty of Science

Bachelor thesis

Functional characterization of succinyl-CoA synthetase in the bloodstream form of *Trypanosoma brucei*

Laboratory of Functional Biology of Protists

Karolína Kubišová

2019

Supervised by RNDr. Alena Panicucci Zíková, PhD

Co-supervised by Bc. Brian Panicucci

České Budějovice

Kubišová K., 2019: Functional characterization of succinyl-CoA synthetase in the bloodstream form of *Trypanosoma brucei.* Bc. Thesis, in English – 47 p, Faculty of Science, University of South Bohemia, České Budějovice, Czech Republic.

Annotation:

During the infectious bloodstream stage (BF), the human pathogen *Trypanosoma brucei* lacks a canonical cytochrome-mediated respiratory chain. Therefore, this form of the parasite depends on the reverse activity of the F_oF_1-ATP synthase to hydrolyze ATP and pump protons into the mitochondrial intermembrane space to maintain the essential membrane potential. The dogma also states that the sole source of organellar ATP is the mitochondrial ADP/ATP carrier, which imports glycolytically derived ATP from the cytosol. In this study, we explore the possibility that the BF mitochondrion is able to contribute to its own pool of consumable ATP by utilizing an active succinyl-CoA synthase to generate ATP *via* substrate phosphorylation.

Declaration:

I hereby declare that I have worked on my bachelor's thesis independently and used only the sources listed in the bibliography.

I hereby declare that, in accordance with Article 47b of Act No. 111/1998 in the valid wording, I agree with the publication of my bachelor thesis, in full to be kept in the Faculty of Science archive, in electronic form in publicly accessible part of the STAG database operated by the University of South Bohemia in České Budějovice accessible through its web pages. Further, I agree to the electronic publication of the comments of my supervisor and thesis opponents and the record of the proceedings and results of the thesis defense in accordance with aforementioned Act No. 111/1998. I also agree to the comparison of the text of my thesis with the Theses.cz thesis database operated by the National Registry of University Theses and a plagiarism detection system.

České Budějovice, 14.8.2019

……
Karolína Kubišová

Acknowledgments

First and foremost, I would like to thank my supervisor, Alena Zíková, for her guidance, wisdom and insight that was invaluable to my research. A special thank you belongs to my co-supervisor, Brian Panicucci, for the enormous amount of time and dedication he had to patiently show me the procedures and walk me through the protocols as well as review my writing. I would also like to express my gratitude to all of the members of the Lab of Functional Biology of Protists who were very kind and friendly and made my stay there enjoyable.

Table of Contents

Abbreviations

AAC – ADP/ATP carrier

ADP – adenosine diphosphate

amp – ampicillin

ASCT – acetate:succinate coenzyme A transferase

ATP – adenosine triphosphate

BF – long slender bloodstream form

bp – base pair

cDNA – complementary deoxyribonucleic acid

CMM – Creek's minimal medium

CoA – coenzyme A

Cp – crossing point value

dH_2O – distilled water

DNA – deoxyribonucleic acid

dNTP – nucleotide

DTT – dithiothreitol

ECL – substrate for enhanced chemiluminescence

ECT – electron transport chain

EDTA – ethylenediaminetetraacetic acid

FBS – fetal bovine serum

G418 – geneticin

GHPhleo – containing geneticin, hygromycin and phleomycin

GTP – guanosine triphosphate

HRP – horse radish peroxidase

IPTG – isopropyl β-D-1-thiogalactopyranoside

LB – lysogeny broth

LN_2 – liquid nitrogen

mRNA – messenger ribonucleic acid

nt – nucleotide

OD_{600} – optical density at 600 nm

OxPhos – oxidative phosphorylation

PAGE – polyacrylamide gel electrophoresis

PCR – polymer chain reaction

PF – procyclic trypomastigote

PVDF – polyvinylidene fluoride

qPCR – quantitative polymer chain reaction

QS – quantum satis

rDNA – ribosomal deoxyribonucleic acid

RNA – ribonucleic acid

RNAi – ribonucleic acid interference

rpm – revolutions per minute

RT – reverse transcriptase

SS-BF – stumpy bloodstream form

SCoAS – succinyl-coenzyme A synthetase

SDS – sodium dodecyl sulfate

siRNA – small interfering ribonucleic acid

SOC – super optimal broth

STE – sodium chloride-tris-EDTA

SubPhos – substrate phosphorylation

TC – tissue culture

TCA – tricarboxylic acid cycle

TetR – tetracycline repressor

UV-Vis – ultraviolet-visible

VSG – variable surface glycoprotein

WCL – whole cell lysate

1. Introduction

Trypanosoma brucei is a flagellated protozoan that causes human African Trypanosomiasis, otherwise known as sleeping sickness, in sub-Saharan Africa. The chronic form of the disease, which comprises 98% of the reported cases, is caused by *T. brucei gambiense* and affects people in 24 central and western African countries (World Health Organization). The parasite is introduced into the mammalian bloodstream after a bite from an infected tsetse fly. During the early stages of disease progression, the symptoms are often elusive or resemble those of a common cold. However, the hallmark symptom of sleeping during the day and insomnolence at night can also be observed in the earlier stages the infection as the circadian rhythm of the host is affected by the human pathogen (Rijo-Ferreira, 2018). Oftentimes, the affected patients live in rural areas with limited access to medical caregivers that can diagnose and effectively treat the disease in the early stages. When left untreated, the parasite eventually crosses the blood-brain barrier and infects the central nervous system.

In contrast, the acute form of the disease is caused by *T. brucei rhodesiense* and is encountered in 13 eastern and southern African countries (World Health Organization). Here the disease manifests very rapidly as the central nervous system is infected much earlier than in the chronic form. Once the parasite crosses the blood-brain barrier, the symptoms become much more severe: personality changes, seizures and difficulty walking and talking. At later stages, the disease can prove fatal. Also, treatment becomes difficult as the drugs capable of crossing the blood-brain barrier are notoriously toxic. Fortunately, the tsetse fly vector has largely been contained through extensive government programs and the number of estimated cases is thought to be below 10,000 (World Health Organization). However, animal Trypanosomiasis or nagana is still a potent threat to these developing countries. The socio-economic impact is devastating, especially to cattle in rural agriculture areas.

In the research lab, we study a causative agent of animal Trypanosomiasis, *T. brucei brucei*, which is not a human pathogen as it is susceptible to a human lytic factor. Just like the closely related human pathogens, it has a complex digenetic life cycle. In the mammalian host, the cells are pleomorphic and exist as either proliferative long slender bloodstream forms (LS-BF) or cell-arrested short stumpy bloodstream forms (SS-BF) (Smith, 2017). Only the SS-BF are pre-adapted for survival in the insect vector. During a tsetse fly bloodmeal, the SS-BF enter the food canal and then differentiate into the procyclic trypomastigote (PF), allowing them to proliferate in the midgut (Dyer, 2013). The parasites eventually migrate

from the anterior part of the midgut to the proventriculus, where the elongated form of the trypomastigote transforms into an epimastigote. Then, a single asymmetric division of the epimastigote results in a long and short form of the parasite. While the long form is generally thought to deteriorate and die, the short form migrates through the foregut to the salivary glands, where it attaches to the epithelium and divides into a cell-arrested metacyclic stage (Sharma, 2009). This form of the parasite then detaches from the epithelium and resides in the lumen of the salivary glands, where it awaits to re-infect a new mammalian host. Upon re-entering the bloodstream, the metacyclic differentiates into the BF parasite, thus completing the life cycle (Smith, 2017).

The LS-BF replicate rapidly by binary fission approximately every 7 hours which enables it to rapidly re-infect the mammalian host. As the cells proliferate and the parasitaemia increases, the cells reach a critical cell density that activates quorum sensing (Mony, 2015). This causes the parasite to differentiate into the non-dividing SS-BF, which serve to prolong the viability of the host and thus increase the chances of transmission to the insect vector. Recently, it was discovered that the extracellular *T. brucei* can also reside in the skin of the mammalian host, which expands the number of sites for transmission (Capewell, 2016). While the parasite employs an elaborate system for antigenic variation to evade the potent mammalian immune system in the blood, the ability to establish newly identified niches in tissues comprised of various types of immune cells may also serve to prolong the infection. These tissue reservoirs (skin, brain and adipose) also present different nutrient microenvironments compared to the glucose abundant bloodstream. This may decrease the rate of proliferation and decrease the virulence of the parasite (Silva Pereira, 2019).

Due to the diverse environments the parasite encounters, the gene expression and metabolism vary dramatically throughout the life cycle. When the PF is grown in a glucose-depleted medium, mimicking the insect midgut, the main carbon source for the energy metabolism becomes proline (Smith, 2017). The amino acid is catabolized and the reduced cofactors generated from the degradation are re-oxidized during oxidative phosphorylation (OxPhos) in the inner mitochondrial membrane (Smith, 2017). The reduced cofactors transfer electrons to the electron transport chain (ETC), which results in the reduction of oxygen and the pumping of protons by complexes III and IV into the intermembrane space (Bringaud, 2006). This forms an electrochemical gradient. As these protons are allowed to flow down this gradient through the proton pore of the F_oF_1-ATP synthase, the potential energy is transformed into mechanical energy to generate chemical energy as the enzyme rotates to

synthesize ATP. The generated ATP can then be exported out of the mitochondrion by an ADP/ATP carrier (AAC) (Smith 2017).

In higher eukaryotes, the electron transport chain is connected to the tricarboxylic acid cycle (TCA) *via* the reduced cofactors produced in the cycle. *T. brucei* possesses all eight genes encoding the TCA enzymes, however their expression varies between life cycle stages (van Weelden, 2005). Interestingly, even though the PF parasite retains the full complement of TCA enzymes, only part of the cycle is actually utilized; namely, the transformation of α-ketoglutarate to succinate in proline degradation and succinate to malate for gluconeogenesis. Acetyl-coenzyme A (acetyl-CoA), which usually feeds the TCA cycle in other organisms, is instead converted to acetate for fatty acid synthesis (Rivière, 2009).

While the PF parasite possesses a well-developed branched mitochondrion with OxPhos, only a tube-shaped reduced mitochondrion is found in the BF parasite. Since, BF *T. brucei* lacks the typical cytochrome-mediated electron transport to power OxPhos, it relies on glycolysis to generate enough cellular ATP. High rates of glycolysis are achieved by isolating the first seven enzymes within the trypanosome specific peroxisome-like organelle called a glycosome (Smith, 2017). There are two ATP consuming steps that are later followed by the formation of two ATP *via* phosphoglycerate kinase in the glycosome. Glycolysis therefore results in no net production of ATP in the glycosome. The remaining three enzymes are located in the cytosol. There, the energetic payoff occurs in the last enzymatic step that generates two ATP by converting two phosphoenolpyruvate molecules into pyruvate *via* pyruvate kinase.

Since the BF parasite lacks the cytochromes for a functional respiratory complex III and IV, the ETC is limited to the glycerol-3-phosphate dehydrogenase and trypanosome alternative oxidase (Zíková, 2017). The glycerol phosphate shuttle utilizes the mitochondrial glycerol-3-phosphate dehydrogenase to convert the glycolytic glycerol-3-phosphate to dihydroxyacetone phosphate. The dehydrogenase then reduces ubiquinone to ubiquinol, which transfers its electrons to a plant-like trypanosome alternative oxidase that reduces oxygen to water. Since the simplified BF ETC doesn't contribute to the essential membrane potential, the F_oF_1-ATP synthase reverses direction and begins to hydrolyze ATP to pump protons into the inter mitochondrial membrane space. The resulting proton motive force is required for mitochondrial protein import. The literature claims that all of the ATP used for this purpose is imported from the cytosol by AAC. The reverse mode of AAC in BF *T. brucei* also contributes electrogenically to the mitochondrial membrane potential as the exchange of

cytosolic ATP^{4-} for mitochondrial ADP^{3-} results in a +1 charge differential. However, some data suggest that the mitochondrion may contribute to its own pool of ATP by utilizing substrate-level phosphorylation (SubPhos) within the mitochondrion (Zíková, 2017).

SubPhos is a process that can generate ATP by transferring a phosphate group from a high energy intermediate substrate to ADP. The reaction is reversible and enzymes called kinases catalyze this transfer. Aside from the glycolytic kinases found in the glycosome and cytosol, *T. brucei* also contains the mitochondrial localized succinyl-coenzyme A synthetase (SCoAS), which is one of the enzymes that comprises the TCA cycle. However, in the BF stage of the parasite, it is believed that the TCA cycle is not active or functional in the traditional sense. Current knowledge of the BF mitochondrion would suggest that SCoAS can potentially participate in two different catalytic pathways, one of which is the following reaction within the proline/glutamine catabolic pathway (Fig. 1):

$$\text{succinylCoA} + \text{ADP} + \text{P}_\text{i} \rightleftharpoons \text{succinate} + \text{CoA} + \text{ATP}$$

Figure 1: Reaction scheme of the conversion of succinyl-CoA to succinate. (ADP – adenosine diphosphate, P_i – inorganic phosphate, CoA – coenzyme A, ATP – adenosine triphosphate).

In *T. brucei*, the SCoAS reaction proceeds predominantly from left to right, generating succinate and ATP (Jenkins, 1988). The metabolic pathway begins when proline or glutamate is first converted into glutamate in the cytosol. The glutamate is then converted into α-ketoglutarate *via* alanine transaminase and the product is transported into the mitochondrial matrix. There, α-ketoglutarate dehydrogenase catalyzes the formation of the succinyl-CoA substrate used for the SubPhos reaction depicted above.

SCoAS is also involved in the threonine/pyruvate catabolic pathways. This unique SubPhos reaction occurs in the *T. brucei* mitochondrion because it possesses the anaerobic enzyme acetate:succinate CoA-transferase (ASCT), which can convert acetyl-CoA, a product from degraded pyruvate or threonine, to the excreted end product acetate (Fig. 2) (Bringaud, 2006). During this process, ASCT transfers coenzyme A from acetyl-CoA to succinate. The cycle is completed when SCoAS regenerates succinate, releasing ATP and coenzyme A.

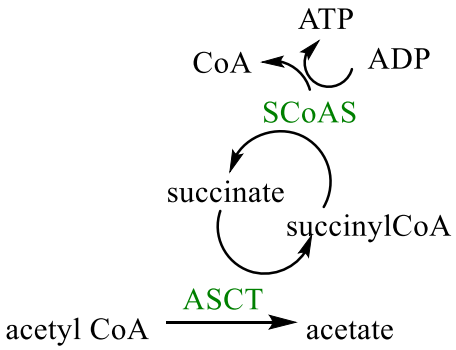

Figure 2: The ASCT/SCoAS cycle. Enzymes are marked in green. (ADP – adenosine diphosphate, ASCT – acetate:succinate CoA-transferase, ATP – adenosine triphosphate, CoA – coenzyme A, P_i – inorganic phosphate, SCoAS – succinyl-coenzyme A synthetase).

The eukaryotic SCoAS is a heterodimer consisting of an α and β subunit. The active sites are located at the region of contact between the two subunits. Both subunits contain the CoA ligase domain, while subunit α also has a Rossman fold domain that binds the CoA substrate. Meanwhile, the mammalian enzyme can synthesize either ATP or GTP, depending on the isoform of subunit β present in the heterodimer (Ostergaard, 2008). In *T. brucei*, SCoAS is also a heterodimer of an α and β subunit. However, there is only one subunit β isoform and it is comprised of an ATP grasp domain, thus it prefers to synthesize ATP over GTP (Jenkins, 1988). Recent transcriptomic and proteomic data indicate that while the overall gene expression is less in BF parasites, both subunits of the SCoAS are present in BF *T. brucei* (Zíková, 2017). Interestingly, studies by *Zhang et al* revealed a severe growth phenotype when the SCoAS β subunit was silenced by RNAi, suggesting that the enzyme is essential to BF *T. brucei.*

While the PF fully branched mitochondrion produces ATP by OxPhos, it has long been considered that the reduced tubular structure of the BF mitochondrion is an ATP consuming organelle. In this thesis, we explore the possibility that ATP generated within the mitochondrion by substrate level phosphorylation may be a source for the ATP consumed by the reverse activity of BF F_oF_1-ATP aside from importing cytosolic ATP derived from glycolysis. The most obvious proof for this hypothesis is the result published in *Zhang et al* that demonstrates that the depletion of SCoAS β is extremely lethal for BF parasites. Therefore, the main focus of this thesis was to reproduce the RNAi silencing of the β subunit and verify the growth phenotype.

2. Aims

Determine if SCoAS is essential in another lab strain of *T. brucei*

- Generate a BF *T. brucei* Lister 427 MiTat 1.2 SCoAS β RNAi cell line
- Verify the RNAi efficiency by qPCR
- Measure the growth phenotype

Prepare *T. brucei* SCoAS β antigen for polyclonal antibody production

- Generate an inducible bacterial cell line that expresses *T. brucei* SCoAS β
- Examine the induced expression levels over time by western blot analysis
- Determine the solubility of the bacterially expressed SCoAS β antigen

3. Methods

3.1. Cultivating cells

We kindly received the properly defined *T. brucei* Lister 427 MiTat 1.2 90-13 cell line from a collaborator. While details about the cell line used in the *Zhang et al* paper were limiting, it was mentioned that some of the cell lines used in their studies were derived from the lab strain that expresses the variable surface glycoprotein (VSG) defined as MiTat 1.2. Since previous SCoAS RNAi cell lines established with our poorly defined Lister 427 lab strain produced contradictory results to the literature, we utilized this alternative lab strain. This cell line was previously genetically modified to introduce the bacteriophage T7 polymerase and the bacterial tetracycline repressor (TetR) into the genome of the parasite, which enables the regulation of RNAi silencing. These cells were grown in HMI-11 media containing 10% fetal bovine serum (FBS). The HMI-11 was prepared from a premixed powder with phenol red as the pH indicator according to the following recipe:

Table 1: HMI-11 + 10% FBS media.

Reagent	**10 L**
Invitrogen HMI-9 premix	181.4 g
Sodium Bicarbonate	30 g
Penicillin/Streptomycin	100 mL
QS with milliQ to:	9.0 L
FBS	1.0 L

This recipe and all of the following recipes found in this thesis were established in the Laboratory of Functional Biology of Protists. In addition to the reagents stated in Table 1, the medium contained the antibiotics G418 (2.5 μg/mL) and hygromycin (5 μg/mL), which act to kill any parasites that do not retain the selectable markers associated with the heterologous expression of the T7 polymerase and TetR from another organism. In this case, the aminoglycoside phosphotransferase gene is coupled with the T7 polymerase and acts to degrade G418. While protection against hygromycin is provided by the hygromycin B phosphotransferase that is included with the TetR.

The trypanosomes were routinely grown in 5 mL cultures in 25 cm^2 flasks. These cultures were kept at a maximal density of 1-2x10^6 cells/mL of culture because at higher densities the cells stop proliferating as they reach the stationary phase of growth. In order to

determine the density and health of a culture, the parasites were monitored under Zeiss Primo Vert optical microscope using a 20X magnification and counted with the Z2 Coulter Counter. Once the culture obtained the maximal density approximately every 2 days, the trypanosomes were split by pipetting out as much of the culture as possible with a 5 mL glass pipette under sterile conditions within the tissue culture (TC) hood. The remnants served as the seeded aliquot of further growth; then 5 mL of fresh media containing antibiotics were added to the flask.

The flasks with the cell cultures were stored in a 37°C incubator with an elevated concentration of CO_2 (5%). This temperature mimics the environment of the mammalian host while the CO_2 along with $NaHCO_3$ in the medium is used to keep the correct pH. This pair works as a buffer to maintain a neutral pH. Due to the need of CO_2, the lids of the flasks were left slightly loose. For routine maintenance of the cell line, the flasks were kept in an upright position. However, a more favorable environment could be created by tilting the flasks almost horizontally to increase the surface area of the culture, thus allowing better aeration.

3.2. Plasmid DNA extraction – Midiprep

The plasmid TbSCoAS p2T7-Phleo (Fig. 3) containing the SCoAS RNAi insert was midiprepped in order to have a sufficient amount of DNA for transfecting BF *T. brucei*. This plasmid was previously generated in the lab to target 600 base pairs (bp) of the SCoAS coding sequence. Double stranded RNAi for the knockdown was created *in vivo* by using head-to-head T7 polymerase promoters flanking the targeted SCoAS sequence. This dsRNAi expression was regulated with a TetR binding sequence located immediately downstream of the promoter. The plasmid also contained a homologous region of the *T. brucei* minichromosome 177 locus that directed the integration of the linearized plasmid through homologous recombination. The plasmid also contains the resistance markers for ampicillin and phleomycin to positively select for bacteria and *T. brucei* harboring the plasmid DNA, respectively. For this experiment, the GenElute HP Plasmid Midiprep Kit was used from Sigma.

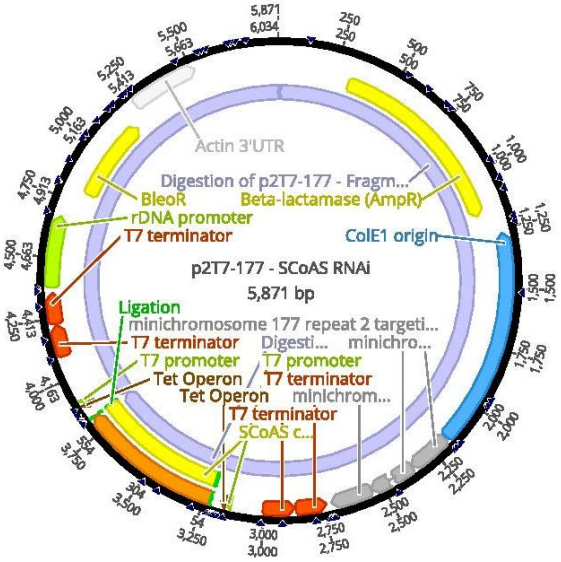

Figure 3: TbSCoASp2T7-phleo plasmid map.

First, a -20 ℃ glycerol stock of previously transformed *Escherichia coli* (*E. coli*) containing the plasmid was thawed and streaked out on a lysogeny broth (LB) agar plate with ampicillin (amp) (Tab. 2). The plate was then incubated at 37°C for not longer than 16 hours to avoid the growth of satellite colonies that do not contain the plasmid. After the incubation, a single colony was selected and grown in 50 mL of liquid LB amp (100 µg/mL) culture in a 37°C vortex incubator spinning at 200 rpm (Tab. 3). Following the incubation of the liquid culture, the bacterial cells were harvested pouring all of the culture into 50 mL conical flasks and spinning them down in a swinging bucket rotor centrifuge at 3,000 x g for 10 minutes. The centrifugation was done at 12°C to prevent enzyme degradation of DNA from lysed cells. After discarding the supernatant, the cells were resuspended in a buffer containing RNAse and then lysed using a lysis buffer, containing alkaline-sodium dodecyl sulfate (SDS). The samples were simply inverted since vortexing would shear the long coils of genomic DNA and these fragments could contaminate the plasmid purification. The sample was neutralized after 3 minutes with a neutralization buffer. Upon the inversion of the flask, a white aggregate containing the precipitated proteins and lipids appeared in addition to the DNA-containing aqueous phase. Before pouring the sample into a filter syringe barrel, a binding solution was added. Once in the barrel, the aggregate was left to rise to the top of the liquid. In the meantime, the binding column, a spin column that is processed in a table-top centrifuge, was prepared by equilibrating the membrane with a column preparation buffer. Subsequently, the plunger was pressed to pass the liquid portion of the solution through the filter and onto the

binding column, thus leaving behind the aggregate. The DNA containing solution was passed through the membrane of the spin column, allowing the DNA to bind to the membrane while all other contaminants were washed through into the collection tube. Then, the DNA was washed using 2 different washing solutions. Placing the spin column in a new collection tube, the elution buffer (preheated to 65°C for better yields) was added to the column to release the plasmid from the membrane. The desired plasmid was then present in the eluate.

Since the transformation procedure of the parasite requires a more concentrated plasmid, an alcohol precipitation step was performed using sodium acetate and isopropanol. After centrifugation, the pellet was washed with cold 70% ethanol. The pellet was left to dry for 5 minutes to remove excess ethanol and then resuspended in the 100 μL of preheated elution buffer. Finally, the concentration of the plasmid DNA was determined using a Nanodrop instrument, a full-spectrum, UV-Vis microvolume spectrophotometer. The elution buffer was used as a blank.

Table 2: LB Agar Plates.

Reagent	**MW or [Stock]**	**500 mL**	**[Final]**
MilliQ		400 mL	
Tryptone		5.0 g	
Yeast Extract		2.5 g	
NaCl	58.45	2.5 g	171 mM
pH ~ 7.3 with NaOH			
QS with milliQ to:		500 mL	
Agar, Bacteriological		7.5 g	
Kanamycin or Ampicillin	50 μg/mL or 100 μg/mL	500 μL	50 μg/mL or 100 μg/mL

Table 3: LB-Luria (0.5 g/L NaCl).

Reagent	**MW**	**500 mL**	**[Final]**
MilliQ		400 mL	
Tryptone		5 g	1%
Yeast Extract		2.5 g	0.5%
NaCl	58.45	0.25 g	85 mM
QS with milliQ to:		500 mL	
pH ~ 7.3 with NaOH			

3.3. Preparing linearized plasmid

Preparing a linearized plasmid facilitates the incorporation of the recombinant DNA into the genome of the parasite. A Not1 restriction site incorporated into the homologous *T. brucei* minichromosome 177 region of the plasmid allows for the linearization of the plasmid. This promotes more efficient homologous recombination that aids in the successful genomic integration of the recombinant DNA. A total of 20 μg of plasmid DNA was digested in the following enzymatic reaction (Tab. 4).

Table 4: TbSCoASp2T7-phleo Not1 linearization digest.

Reagent	**50 μL**
Plasmid (20 μg)	6.6 μL
MilliQ	33.4 μL
10x FD buffer	5 μL
Not1 FD	5 μL

This mixture was incubated at 37°C for 2 hours. Subsequently, 3 M sodium acetate with a pH of 5.2 was added along with ice cold 96% ethanol to precipitate the DNA. The sodium acetate was required to neutralize the negative charge of the DNA. The mixture was then vortexed and left in -80°C for half an hour. Subsequently, the plasmid was spun down at 4°C for 30 minutes and the supernatant was removed with an aspirator. The pellet was then washed with 70% ethanol to remove abundant quantities of salt. In the meantime, sterile milliQ water was preheated to 65°C before it was used to resuspend the DNA pellet under sterile conditions. The concentration of the resulting DNA was quantified using the Nanodrop.

To verify the successful linearization of the plasmid DNA, a small aliquot of both digested and undigested plasmid were resolved on an agarose gel when an electric current was applied. This method separates the negatively charged DNA fragments by size as smaller molecules pass more easily through the lattice formed by the solidified agarose. A 0.8% agarose gel was prepared with the intercalating dye ethidium bromide to visualize the DNA (Tab. 5).

Table 5: 0.8% Agarose Gel.

Reagent	Amount
Agarose	0.56 g
0.5x TAE	70 mL
Ethidium Bromide	1 µL

Prior to loading the plasmid on the gel, a 10x DNA loading dye containing glycerol (Tab. 6) was added to the sample and thoroughly homogenized to ensure that the DNA would sink into the well of the gel. The loading dye also contains the negatively charged detergent SDS, which acts to denature the DNA and provide a uniform charge to the molecule. An aliquot of a DNA ladder (Fig. 4) containing molecules of known sizes was loaded as a reference. Once the remaining samples were loaded onto the gel, a voltage of a 100 V was applied. The wells of the agarose gel are located near the negatively charged cathode of the apparatus, which repels the negatively charged DNA and causes it to migrate down the gel. Since it is easier for smaller DNA molecules to navigate the pores of the agarose lattice, the smaller molecules will migrate the farthest. After 45-60 minutes of applying the constant voltage, we used the UV light from the Chemidoc Gel Imaging System (BioRad) to visualize the gel with the ImageLab software.

Table 6: 10x DNA loading dye.

Reagents	MW or [Stock]	10 mL	[Final]
MilliQ		4.2 mL	
Glycerol	80%	4.9 mL	39%
SDS	10%	500 µL	0.5%
EDTA	0.5 M	200 µL	10 mM
Xylene cyanol	2%	250 µL	0.1%

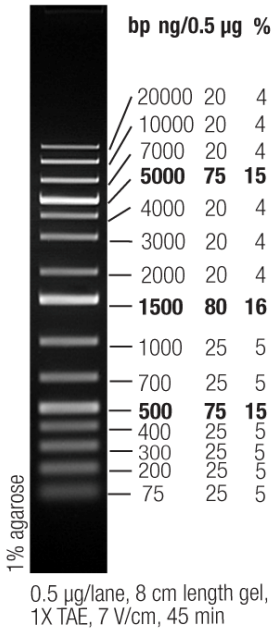

Figure 4: 1 kb Plus DNA Ladder.

3.4. BF *T. brucei* transfections & selection

To coax the BF parasite to uptake and incorporate the linearized plasmid DNA, the cells were electroporated during the transfection process. In preparation for the transfections, the culture was expanded in order obtain a final amount of $3x10^7$ cells. In our case, we required double that amount as we also included a mock transfection using sterile milliQ water instead of the linearized plasmid DNA as a negative control experiment. Since it is critical that the cells remain in the mid-log phase of growth (between $0.6\text{-}0.8x10^6$ cells/mL) to promote active replication, a 100 mL culture was prepared. The cells were harvested in two 50 mL conical flasks and spun in a swinging bucket rotor centrifuge for 10 minutes at 1,300 x g. Then the pellets were washed once with sterile phosphate-buffered saline (Tab. 7) supplemented with (6 mM) of glucose (PSB-G) (Tab. 8). The added glucose provides a carbon source to keep the trypanosomes viable.

Table 7: PBS buffer.

Reagent	[Stock]	1 L	[Final]
MilliQ		700 mL	
Sodium Phosphate, pH 8.0	0.1 M	200 mL	20 mM
NaCl	5 M	100 mL	500 mM

Table 8: PBS-G buffer.

Reagent	MW or [Stock]	500 mL	[Final]
MiliQ		450 mL	
PBS	10x PBS	50 mL	1x
Glucose	180.16	541 mg	6 mM

Subsequently, each cell pellet was resuspended in an AMAXA Human T-cell solution chilled to 4°C. This solution contained 81.8 µL of the Human T-cell nucleofector solution mixed with 18.2 µL of the AMAXA supplement. 100 µL of the cell suspension was added to a 0.2 cm gap cuvette (BioRad) that contained either 12 µg of linearized plasmid DNA or milliQ water. Both samples were then electroporated using the X-001 program on the AMAXA Nucleofector II electroporator.

The electroporated cells were subsequently serially diluted with the aim of creating near clonal cell lines that would be populated with parasites consisting of almost identical genetic information having arisen from just a few cells. For each electrocuvette, three 50 mL conical tubes were prepared, with the first tube (A) containing 30 mL of HMI-11 medium along with G418 (2.5 µg/mL) and hygromycin (5 µg/mL). Due to the stress of the electroporation, the cell cultures were allowed to recover for 16 hours before adding phleomycin, the selectable marker for the plasmid DNA that is targeted for genomic integration. The remaining tubes (B and C) were filled with 27 mL of the same medium and antibiotics. The whole content of the electrocuvette was then transferred into tube A. That tube was then inverted several times to ensure that the cells are well distributed, diluting them to a concentration of $1x10^6$ cells/ml. Then, 3 mL from the tube A were transferred to tube B. The steps were repeated again for tube B – resulting in a final concentration of $1x10^5$ cells/mL – and later for tube C – with a final concentration of $1x10^4$ cells/mL – for both the mock sample and the sample containing the target DNA sequence. Then 1 mL aliquots were distributed from each dilution (tubes A, B and C) onto a 24 well plate, resulting in a total of 3 plates for the mock and 3 plates for the SCoAS RNAi transfected cells.

The next day, phleomycin was added to the plates of transfected cells to begin selecting positive cell lines. 1 mL of HMI-11 medium containing G418 (2.5 µg/mL), hygromycin (5 µg/mL) and a 2x concentration of phleomycin (5 µg/mL) was added to every well containing 1 mL of plated parasites. Once the genetically modified parasites recovered and started actively dividing again, the medium became depleted of nutrients and they needed to

be split. Since there were many dead cells in each well that could negatively affect the growth of the transfected parasites, it was necessary to transfer the cells to an empty well. At first, the cells were diluted 1:3 by taking 500 µL of the old culture and adding 1 mL of the new HMI-11 GHPhleo medium. As the trypanosomes continued to proliferate, they were diluted 1:5. Finally, six positive transfectants were selected for further experiments and diluted 1:10 into a new 25 cm^2 flask.

3.5.Creating stabilates

In case of further use of the clones in the future, stabilates of the non-induced clones were made. The stabilates allow the cells to be conserved over longer periods of time without changing their metabolism. These stabilates were prepared under sterile conditions by mixing 500 µL of the Bloodform Freezing solution (Tab. 9) and 500 µL of the cell culture into an individual cryovial for each clone. Ideally, the cells should be dense and near the top end of the mid-log phase, with a cell density around $1.2x10^6$ cells/mL. The parasites were slowly cooled by placing the cryovials on ice for half an hour, followed by storage in -80°. Three days later, the stabilates were transferred to liquid nitrogen tanks.

Table 9: Bloodform Stabilate Freezing solution.

Reagent	MW or [Stock]	500 mL	[Final]
MilliQ		200 mL	
Glucose	180.16	9.3 g	100 mM
NaCl	58.44	2.1 g	72 mM
Sodium Citrate	294.1	0.75 g	5 mM
BSA	66.78	0.5 g	15 mM
Glycerol	80%	75 L	12%

3.6. Growth Curves

One assay used to determine if a gene product is essential involves measuring and comparing the growth rate of an uninduced RNAi cell line to the same cell line depleted of the protein. A total of 3 clones – B5, BC5 and C5 – were selected to screen for variability between clones. Each clone was split into 2 flasks, one of which was induced for RNAi with the addition of 1 µg/mL tetracycline while the other served as a negative control. The addition of tetracycline served to bind the TetR, causing a conformational change to the protein that

releases it from DNA element downstream from the T7 RNA polymerase promoter. This essentially removes the steric hindrance of the polymerase and the transcription of the complementary sequence to the SCoAS sequence is initiated, thus turning on the RNAi silencing. The aim of this experiment was to see whether the rate of proliferation decreases over time in the induced cells. To visualize this correlation between the proliferation rate and time, we recorded the cumulative density. This approach simulates an ideal situation where the parasites could grow continuously in one infinitely large flask without the need for splitting the culture, thus resulting in a linear figure.

This cumulative density was calculated by measuring the density of the cells every day over the course of 7 days. The previously mentioned Z2 Coulter Counter was used to count the cells and determine the concentration of the cultures. On day 0 of the growth curve, the cells were seeded to $2x10^5$ cells/mL in 5 mL of HMI-11 GHPhleo medium either containing tetracycline or not. Every day the cell cultures were counted and it was calculated how much of the culture should remain so that it would again have a concentration of $2x10^5$ cells/mL (Eq. 1). Fresh tetracycline was included in the media used to split the induced cultures each time. The dilution factor for each culture was also calculated according to Eq. 2. A running total of the daily dilutions of a culture was calculated by multiplying each day's dilution factor by the product of all the previous dilution factors, yielding the cumulative dilution factor (Eq. 3) at each time point. Once all the values were known, the density of the cells on a specific day was multiplied by the cumulative dilution factor of that day, resulting in the cumulative density. In the end, the cumulative density vs time was plotted on a graph in Excel.

$$V_{seeding} = \frac{2 \times 10^5\ cells/ml}{c_{measured}}$$

Equation 1: Volume of old culture needed for seeding.

$$dilution = \frac{5\ ml}{V_{seeding}}$$

Equation 2: Cell culture dilution.

$$\rho_{cumulative} = \prod_{day\ n}^{day\ 1} dilution \times c_{measured}$$

Equation 3: Cumulative density.

3.7. qPCR analysis

The efficiency of the induced RNAi cell line to deplete the SCoAS β transcript can be determined by performing quantitative polymerase chain reaction (qPCR). This analysis contains 4 steps: 1) harvesting total *T. brucei* RNA, 2) DNase treatment, 3) reverse transcriptase, and 4) the actual qPCR. In order to monitor the targeted SCoAS β RNA depletion, three time points were chosen: day 0, day 2 and day 4 after tetracycline induced RNAi.

T. brucei total RNA was isolated using the RNeasy Mini Kit as described by the manufacturer (Qiagen). 1-2x10^8 cells were harvested in two balanced 50 mL conical tubes that were spun at 8°C for 10 min at 1,300 x g in a swinging bucket rotor. The cell pellet from both conicals was thoroughly resuspended in a total of 1 mL of PBS-G (Tab. 8) and transferred to a 1.5 mL Eppendorf tube. The cells were spun down once again under the same conditions, except this time the microcentrifuge was maintained at room temperature. All of the following spins were also carried out at room temperature. After the spin, all of the supernatant was thoroughly removed with an aspirator. The cell pellet was resuspended in 600 µL of the cell lysis buffer RLT. Afterwards, 600 µL of 70% ethanol was added and the sample was mixed well by pipetting. The cell lysate was then transferred to a spin column housed in a 2 mL collection tube and centrifuged for 15 seconds at 8,000 x g to bind the RNA to the silica-based membrane of the column. Since the maximum capacity of the column is only 700 µL, the remaining cell lysate needed to be applied in a subsequent step. Using the same centrifuge settings, the column was then washed once with 700 µL of RW1 buffer and then twice more with 500 µL RPE buffer. To remove any residual ethanol from the RPE buffer, the last wash was performed for 2 minutes at 8,000 x g. Then the spin column was placed in a new collection tube without any wash buffer and centrifuged for 1 minute at 8,000 x g. Finally, the column was placed in another fresh collection tube and eluted with 50 µL RNase-free water by spinning the column for 1 minute at 8,000 x g. The quality and concentration of the eluted RNA was measured on the Nanodrop. Since the RNA was immediately processed for the downstream applications of qPCR, the RNA sample was stored at -20°C. The remaining unprocessed RNA was then stored for long-term storage at -80°C.

Single-stranded mRNA is very unstable compared to double-stranded DNA. To further analyze the amount of a specific transcript, we need to reverse transcribe it to cDNA. However, any remnants of the cell's DNA will contaminate the RNA and affect our results.

Therefore, we employed the TURBO DNA-free Kit from Invitrogen to first treat the RNA with an exonuclease that degrades DNA. Per the manufacturer's recommendations, a 50 µL reaction was prepared with 10 µg of RNA, 5 µL of a 10x buffer, 1 µL Turbo DNase and nuclease-free water. After thorough mixing, the reactions were incubated at 37° for 30 minutes. Contaminating proteins and small DNA molecules were then removed from the RNA samples with the RNeasy MinElute Cleanup Kit from Qiagen. Spin columns from the kit were stored in at 4℃ and 150 µL of RNase-free water was preheated to 65°. Following the manufacturer's guidelines, the volume of the DNase treated RNA samples was adjusted to 100 µL with RNase-free water before adding 350 µL of RLT buffer. Then 250 µL of 96% ethanol was added and the resulting solution was mixed well by pipetting before it was immediately transferred to a spin column and centrifuged for 30 seconds at 8,000 x g at room temperature as were all of the following spins. The column was placed into a new collection tube and 500 µL of RPE was added. The sample was centrifuged under the same conditions as before and the flow-through was discarded. 500 µL of 80% ethanol was added and centrifuged for 2 minutes. To remove any remaining ethanol, the column was transferred to a new collection tube and the lid of the tube was left open as it was spun for 5 minutes at 16,000 x g. Finally, the column was placed into a new collection tube and the RNA was eluted in 14 µL of pre-warmed RNase-free water.

For the reverse transcriptase reaction, it is essential to transcribe all of the harvested total RNA in an unbiased manner. For this purpose, we utilized the random hexamers supplied with the TaqMan Reverse Transcription Kit (Life Technologies) to act as primers to anneal to any RNA molecule and promote the transcription of cDNA without favoring any specific regions of RNA. The user manual stipulated that each 20 µL reaction should contain the following: RNase free water, 2 µL of 10x RT buffer, 1.4 µL of 25 mM $MgCl_2$, 4.0 µL of 10 mM dNTP mix, 1.0 µL of RNase inhibitor, 1.0 µL of Multiscribe reverse transcriptase and 1.0 µL of 50 µM random hexamers. These reagents were assembled into two master mixes, one with the reverse transcriptase enzyme and one without, the later acting as a control to determine the extent of DNA contamination in each cDNA sample. All of the reagents were kept on ice. Finally, each reverse transcription reaction was prepared in a PCR tube by combining 14 µL of a master mix and 2 µg of total RNA diluted to a final a volume of 6 µL. The reaction ran for 10 minutes at 25°C for the annealing step, followed by a half hour at 37°C for the elongation step. Then the denaturation step ran for 5 minutes at 95°C. After these

steps were finished, the reaction sample was kept at 4°C until the tubes were removed and stored at -20°C.

The aim of the qPCR reaction is to quantify the amount of SCoAS β transcript relative to the abundance of a reference transcript at different time points of RNAi induction. Ideally, the reference transcripts should be involved in unrelated biology processes from the target transcript and thus display minor variability between samples. To calculate how efficiently the induced RNAi depleted the target transcript, we compared the relative abundance of the SCoAS β transcript to the reference transcript of ribosomal 18S at day 0, day 2 and day 4 post SCoAS RNAi induction. We also included a control in which the RNA sample was not transcribed to cDNA due to the omission of the reverse transcriptase. This control would be used to verify that the amount of contaminating DNA in a sample was not enough to interfere with the interpretation of the qPCR data. The clone B5, of the BF Lister 427 MiTat 1.2 SCoAS β RNAi cell line was analyzed by qPCR in a 96 well PCR plate. The manual accompanying the LightCycler 480 SYBR Green I Master Mix (Roche) specified that each 20 μL qPCR reaction consist of 2 μL of cDNA, 10 μL of 2x SYBR Green I master mix (FastStart Taq DNA Polymerase and a DNA double-strand-specific SYBR Green I dye) and 4 μL of both the forward and reverse 1.5 μM primers (Tab 10.).

Table 10: Primer sequences for qPCR of the TbSCoAS p2T7-Phleo plasmid.

Name	Sequence
AZ0704	GGTATCGTTGCGGCGTCT
AZ0705	CGCTTGCCTTCTTCTTCCTTG

The cDNA was diluted 1:4 for the target SCoAS β qPCR reactions and 1:500 for the highly abundant reference transcript. The control qPCR reactions that included template generated without the reverse transcriptase were diluted as previously stated depending on the transcript being amplified. To address possible loading errors in this highly sensitive assay, each transcript at each time point was analyzed in triplicate, with the exception of the control reactions to monitor genomic DNA contamination. Upon the addition of the final reagent, the reactions in each well were mixed well by pipetting. Then a plastic foil cover was evenly adhered to the top of the 96 well plate, which was then spun for 2 minutes at 200 rpm at room temperature. Finally, the plate was loaded into the LightCycler 480 Instrument (Roche).

3.7.1. Quantification of qPCR data

The amount of amplified DNA from each well is determined by measuring the fluorescence from the SYBR Green dye during each cycle of the qPCR reaction. The cycle number and fluorescence values are then extracted from the LightCycler 480 and exported to an Excel spreadsheet, where the raw data can be used for further mathematical manipulations. The first calculation involves the program LinRegPCR to calculate the PCR efficiency of each primer set using linear regression. This value represents the efficiency of the primers to anneal to the target sequence and for the polymerase to amplify it. In an ideal situation, the efficiency would be equal to 2 as the amount of DNA would double after one cycle. However, PCR primer pairs are rarely this efficient, so it is important to factor this into the equations when we compare the amount of DNA amplified using different primer sets. Once the PCR efficiencies for each primer set were calculated, they were entered into the software included with the LightCycler 480 to calculate the crossing point value, Cp. The amplification curve of a qPCR reaction has 3 distinct regions: the region when the fluorescence does not exceed the background fluorescence, the exponential region, and the plateau region when the reagents are depleted. An arbitrary but constant fluorescence threshold value that crosses through the exponential phase of each qPCR reaction is selected. Then the software calculates the cycle number or Cp value where the fluorescence crosses this threshold in each sample. Finally, the Cp and PCR efficiencies are inserted into the following formula (Pfaffl, 2001):

$$\frac{(Cp_{target}\ untreated - Cp_{target}\ treated)^{efficiency\ target}}{(Cp_{reference}\ untreated - Cp_{reference}\ treated)^{efficiency\ reference}}$$

Equation 4: Pfaffl calculation.

Here, the target untreated Cp value is for the fluorescence measured from the SCoAS β amplicon generated from the cDNA produced from the uninduced SCoAS β RNAi cell line. Whereas the target treated Cp value is derived from the SCoAS β fluorescence measured in the RNAi cell lines induced for two or four days with tetracycline. The efficiency target is the PCR efficiency calculated for the SCoAS primers. Finally, the Cp reference refers to the fluorescence values detected from the ribosomal 18S amplicon in the noninduced and RNAi induced samples. These values depict how well the SCoAS β transcript was depleted after two or four days of induced RNAi compared to the levels of transcript present in the noninduced RNAi samples.

3.8.TbSCoAS antigen preparation

3.8.1. Plasmid DNA extraction - Miniprep

The second phase of the thesis involved the initial steps of bacterial expression and purification of the *T. brucei* SCoAS β protein. The goal was to use this protein as an antigen in rabbits to develop an antibody that could detect SCoAS β in western blot analyses of *T. brucei* whole cell lysates. For this, we utilized the bacterial expression plasmid pSKB3 that was previously cloned to contain the 1257 nt of the SCoAS coding sequence (Fig. 5). To purify the recombinant protein, the plasmid included a 6x histidine (6-His) tag that was fused at the N-terminus of SCoAS β. Furthermore, this plasmid includes the neomycin phosphotransferase II gene, which confers resistance to kanamycin and acts as a positive selectable marker in bacteria that contain the plasmid.

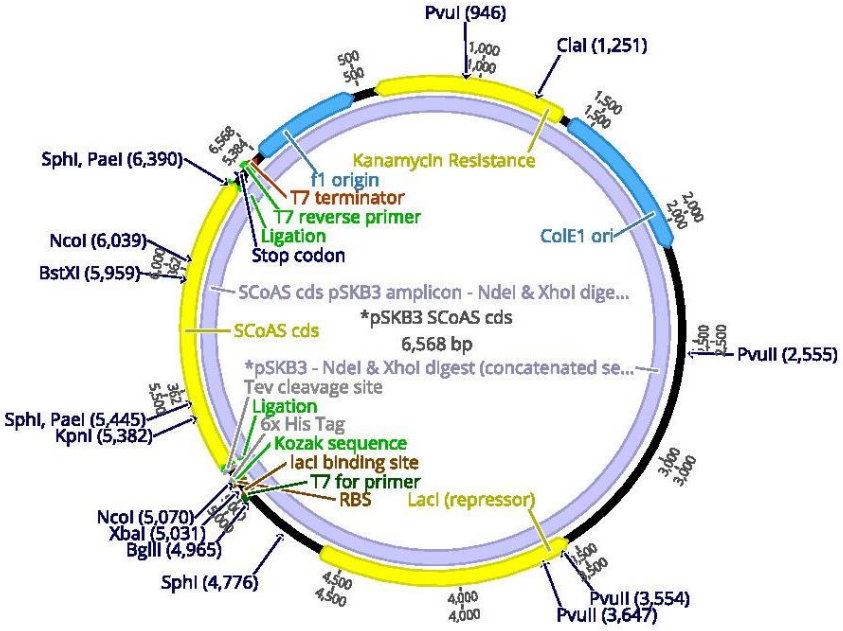

Figure 5: pSKB3 plasmid map.

The previously cloned SCoAS β pSKB3 vector was stored as a bacterial glycerol stock of XL1-blue *E. coli*, an excellent host strain for routine cloning applications. Therefore, we used the GenElute HP Plasmid Miniprep Kit (Sigma) to isolate the plasmid from a bacterial culture grown overnight at 37°C in 5 mL LB media (Tab. 3) containing 50 µg/ mL kanamycin. A total of 4.5 mL of bacteria were harvested in 1.5 mL aliquots by centrifugation at room temperature for 1 minute at 16,000 x g. After the final spin, the supernatant was

aspirated and the cell pellet was resuspended in 200 μL resuspension buffer that was chilled to 4°C. Subsequently, the cells were lysed by adding 200 μL lysis buffer and gently inverting the tube 6-8 times before incubating for no more than 5 minutes. After that, 350 μL of neutralization buffer was added and the tube was gently inverted 4-6 times so as to not shear any of the genomic DNA. The sample was then spun for 10 minutes at 16,000 x g. These steps caused all of the cellular membranes and proteins to precipitate, leaving the DNA in the supernatant. In the meantime, 500 μL of column preparation solution was added to the spin column, which was centrifuged for 1 minute at 16,000 x g at room temperature as were all of the following spins. Once the flow-through was discarded, the cleared lysate was transferred to the spin column and centrifuged for 1 minute at 16,000 x g. The desired plasmid was now bound to the membrane of the column. Therefore, the flow-through was discarded after the following wash spins. The sample was washed once with 500 μL of wash buffer 1 and then with 750 μL of wash buffer 2 using the previously stated centrifugation parameters. The column was spun once more without adding any additional wash buffer to remove any traces of ethanol. The spin column was transferred to a new collection tube and the plasmid DNA was eluted in 50 μL of elution buffer preheated to 65°C. Again, this step involved a spin for 1 minute at 16,000 x g. The concentration and purity of the isolated plasmid DNA was determined on the Nanodrop.

3.8.2. Restriction digest and sequencing

To ensure that the plasmid contained the crucial SCoAS β coding sequence, a restriction digest analysis was performed with NdeI and XhoI, since these restriction sites flanked the 5' and 3' ends of the SCoAS β coding sequence, respectively. A 50 μL digest, consisting of 700 ng of plasmid, 5 μL of 10x buffer and 1 μL of NdeI and XhoI was incubated at 37°C for 15 minutes. Then, the sample was resolved on a 0.8% agarose gel at 100 V for 45 minutes. The ethidium bromide stained gel was visualized using the ImageLab software on the Chemidoc gel imaging system (BioRad). The plasmid (500 ng) was also sequenced by SeqMe (Prague) using 25 pmol of opposing plasmid specific primers (5 μM) (Tab 11.) that provide 2x coverage of the SCoAS β coding sequence.

Table 11: Primer sequences for sequencing the pSKB3 plasmid.

Name	Sequence
AZ0789	CGCGCATATGTTTACTCGCATTGGTCG
AZ0790	ATACTCGAGTTACGCGGCGAGTTTGCATG

3.8.3. *E. coli* competent cell preparation

For the bacterial expression, we used C41 *E. coli* cells that were derived from BL21 (DE3) bacteria. These genetically modified cells contain the T7 RNA polymerase to drive protein expression, but the polymerase is regulated by a mutated lacUV5 promoter that upon induction results in much lower amounts of T7 RNA polymerase than in BL21 (DE3) cells. In order to coax the bacteria to uptake the foreign pSKB3 plasmid, we need to make them competent, i.e. the addition of calcium chloride creates pores in the cell wall.

All of the following steps were carried out in sterile conditions. First, 5 mL of LB (Tab 3.) media was inoculated with C41 cells stored at -80°C and left in the shaking incubator at 37°C overnight. The following day, 1 mL of the bacterial culture was added to 50 mL of new LB media. The cells were left in the 37°C shaking incubator until the OD_{600} reached 0.4, which took an hour and a half. The whole culture was then transferred to 50 mL conical flasks and the cells were centrifuged at 8000 rpm for 10 minutes at room temperature. After pouring off the supernatant, the pellet was resuspended in cold 0.1 M $CaCl_2$. The cells were left on ice for 30 minutes and then spun again as before. The pellet was resuspended once more in 4 mL of 0.1 M $CaCl_2$. Finally, the cells were stored at 4°C, where they remain competent for up to 10 days.

3.8.4. *E. coli* transformation

Subsequently, the perforated C41 cells were transformed by incorporating the pSKB3 genetic information. The heat shock transformation method was used for this purpose. 1 μL of plasmid was added to 100 μL of cells and they were incubated on ice for 12 minutes. The cells were then heat shocked in a 42°C water bath for 45 seconds. Then they were kept on ice for 2 minutes to recover. Then 200 μL of the rich bacterial media SOC (Tab. 12) was added and the bacteria were incubated in a 37°C shaking incubator for 45 minutes. The bacteria were then plated out on LB plates (Tab. 2) containing 50 μg/mL of the selectable marker kanamycin and then placed in a 37°C incubator overnight.

Table 12: SOC medium.

Reagent	MW or [Stock]	50 mL	[Final]
Yeast Extract		0.250 g	0.5%
Tryptone		1 g	2%
NaCl	5 M	100 µL	10 mM
KCl	1 M	125 µL	2.5 mM
$MgSO_4 \cdot 7H_2O$	246.48	0.123 g	10 mM
$MgCl_2 \cdot 6H_2O$	203.30	0.102 g	10 mM
Glucose	180.15	0.180 g	20 mM
MilliQ		40 mL	

3.8.5. Lysozyme Solubility Assay

Next, we performed a solubility assay to determine if the expressed SCoAS β protein is soluble, a crucial factor that dictates how the protein can be purified.

The transformed C41 bacterial cells were grown overnight in a 5 mL LB culture containing kanamycin. 1 mL of the culture was spun down the following day at 5000 x g for 5 minutes at room temperature. All of the following spins were also performed at room temperature. The pellet was resuspended in 1 mL of fresh LB and transferred to a 250 mL flask containing 50 mL of LB media with 50 µg/mL kanamycin. The bacterial culture was then incubated in the 37°C shaking incubator. In the meantime, the STET lysis buffer was prepared (Tab. 18). Once the OD of the cells reached about 0.6, 1 mL of the culture was removed and placed into an Eppendorf tube to create a whole cell lysate (WCL) sample of the uninduced cells. These cells were subsequently spun down for 5 minutes at 5000 x g. The resulting pellet was resuspended in 100 µL of PBS (Tab. 7) before 50 µL of 3x SDS-PAGE sample buffer (Tab. 13) was added. To thoroughly denature the proteins, the sample was boiled at 97°C for 7 minutes. The whole cell lysate was then allowed to cool to room temperature for a few minutes before it was stored at -20°C.

Table 13: 3x SDS-PAGE sample buffer.

Reagent	MW or [Stock]	Amount	[Final]
SDS	20%	9 mL	6%
DTT	154	1.4 g	300 mM
Tris pH 6.8	1 M	4.5 mL	150 mM
Glycerol	80%	11.25 mL	30%
Bromophenol Blue	2%	300 µL	0.02%
QS with MilliQ			30 mL

The remaining bacterial culture from the 250 mL flask was induced to express the *T. brucei* SCoAS β with the addition of 50 µL 1 M IPTG (Tab. 15). After an hour incubation in the 37℃ shaking incubator, samples were collected to prepare whole cell lysates and test for solubility. Whole cell lysates were prepared from 1 mL of the bacterial culture as described above. In addition, 2 mL of cells were also removed for the solubility assay. These samples were spun the same as the whole cell lysates and the supernatant was discarded. Then the pellet was flash frozen in liquid nitrogen and left to thaw on ice for 5 minutes. Then the cell pellet was resuspended in 150 µL of STE (Tab. 17) before being mixed with 150 µL of the STET lysis buffer. Finally, 30 µL of 10 mg/mL lysozyme (Tab. 14) was added and the sample was briefly vortexed before being incubated at 37°C for 30 minutes. The release of the genomic DNA makes the lysed cells very viscous, so the sample is DNased treated by adding 1 µL of 1 M $MgCl_2$, 2 µL of 0.1 M $CaCl_2$ and 2 µL of 1 mg/mL DNase I (Tab. 16). Then the samples were rotated for 15 minutes at room temperature before they were centrifuged at 10,000 x g for 30 minutes at 4°C. The supernatant was transferred to a new Eppendorf tube, while the remaining pellet was resuspended in 335 µL of STET (same volume as supernatant). 167.5 µL of SDS 3x loading dye was added to both the supernatant and pellet. The samples were then boiled at 97°C for 7 minutes and then stored in 20°C. This was repeated for samples harvested after 2 and 3 hours of bacterial expression.

Table 14: 10 mg/mL Lysozyme solution.

Reagent	[Stock]	5 mL	[Final]
MilliQ		4.5 mL	
Tris-HCl, pH 8.0	1 M	50 µL	10 mM
Lysozyme	powder	50 mg	10 mg/mL
QS with milliQ to		5 mL	

Table 15: 1 M IPTG solution.

Reagent	MW	10 mL	[Final]
MilliQ		7 mL	
IPTG	238.1	2.4 g	1 M
QS with milliQ to		10 mL	

Table 16: 10 mg/mL DNase I.

Reagent	[Stock]	1 mL	[Final]
MilliQ		345 µL	
Tris-HCl, pH 7.5	1 M	10 µL	10 mM
NaCl	5 M	10 µL	50 mM
$MgCl_2$	1 M	10 µL	10 mM
DTT	1 M	1 µL	1 mM
Glycerol	80%	625 µL	50%
DNase I	powder	10 mg	10 mg/mL

Table 17: STE buffer.

Reagent	[Stock]	100 mL	[Final]
MilliQ		91.8 mL	
Tris-HCl, pH 8.0	1 M	5 mL	50 mM
NaCl	5 M	3 mL	150 mM
EDTA	500 mM	200 µL	1 mM

Table 18: STET buffer with Triton 2%.

Reagent	[Stock]	100 mL	[Final]
MilliQ		72.8 mL	
Tris-HCl, pH 8.0	1 M	5 mL	50 mM
NaCl	5 M	3 mL	150 mM
EDTA	500 mM	200 µL	1 mM
Triton X-100	10%	20 mL	2%

3.8.6. SDS-PAGE

Sodium dodecyl sulfate (SDS) polyacrylamide gel electrophoresis (PAGE) is a method used for the separation of denatured proteins according to their size. The SDS coats the surface of the protein with a negative charge, which then migrates down the polyacrylamide gel from the cathode toward the anode. In this case, the gel is placed vertically and the smaller the protein, the farther down the gel they will migrate as they encounter less resistance from the polyacrylamide lattice. In our experiments, all of the SDS-PAGE gels used were Any kD Mini-PROTEAN TGX Precast Protein Gels (4-12%) gels from BioRad. Before each run, the wells were washed out with SDS-PAGE running buffer (Tab. 19). The first well always contained 4 µL of the PageRuler protein ladder (Thermo Fisher Scientific) for protein size comparisons (Fig. 6 & 7). The gels ran at 130 V until the blue dye in the samples ran out of the gel.

Table 19: SDS-PAGE running buffer.

Reagent	MW	1 L	[Final]
MilliQ		70 mL	
Tris	121.14	3.03 g	25 mM
Glycine	75.07	14.44 g	192 mM
SDS	280.4	1 g	0.1%
QS with MilliQ		1 L	

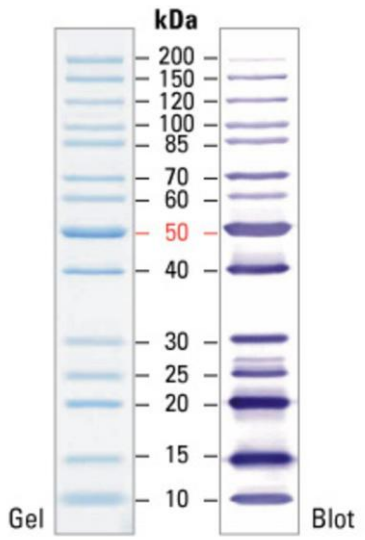

Figure 6: PageRuler Unstained Protein Ladder used for Coomassie staining**.**

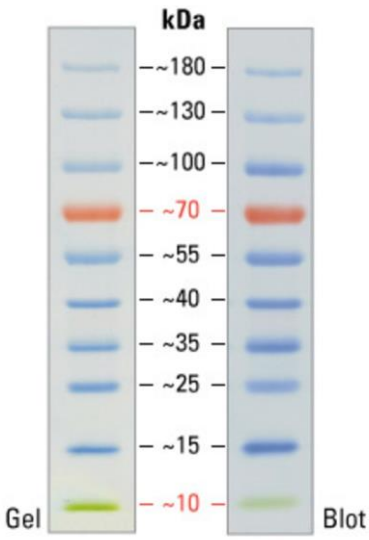

Figure 7: PageRuler Prestained Protein Ladder used for western blot**.**

3.8.7. Coomassie staining

An SDS-PAGE gel can be stained with Coomassie to visualize all the proteins present. Since the bacterial protein translation machinery is usually co-opted to produce large quantities of the heterologous protein compared to its own proteome, the protein of interest is often visible as a robust drop-out band in a Coomassie stained gel. Therefore, to visualize if the bacterial expressed SCoAS β was soluble or not, an SDS-PAGE gel was loaded with the unstained protein ladder and samples from whole cell lysates, pellets and supernatants prepared at various timepoints during the induction. The running conditions for the SDS-PAGE gel was the same as previously stated. Once the run was finished, the gel was placed on an orbital shaker and rinsed in distilled water for 5 minutes. The water was discarded and the gel was then incubated with a fixing solution (Tab. 20) for half an hour. Then the fixing solution was discarded and the gel was stained with Coomassie (Tab. 21) for 20 minutes on the orbital shaker. Once the stain was removed, the gel was rinsed twice with distilled water. Finally, destaining solution (Tab. 22) was poured into the container in excess to destain the gel. A paper towel was also added to help absorb the stain. The gel was left on the shaker overnight. The following morning the gel was imaged on the Chemidoc.

Table 20: Fixing solution.

Reagent	500 mL	[Final]
dH_2O	200 mL	
Methanol	250 mL	50%
Acetic acid	50 mL	10%

Table 21: Coomassie dye solution.

Reagent	500 mL	[Final]
Methanol	250 mL	50%
Coomassie R-250	0.5 g	0.1%
MilliQ	200 mL	
Acetic acid	50 mL	10%

Table 22: Destaining solution.

Reagent	1 L	[Final]
dH_2O	880 mL	
Methanol	50 mL	5%
Acetic acid	70 mL	7%

3.8.8. Western blot

To definitely determine if the bacterial expressed SCoAS β protein was present in the soluble or insoluble fractions, we performed a western blot analysis. Since the recombinant SCoAS β contained a 6x histidine tag, it was possible to selectively visualize the resolved protein using a monoclonal antibody that recognizes this epitope tag.

After whole cell lysates and the soluble and insoluble fractions for each time point were resolved by SDS-PAGE, the proteins were transferred to a more stable PVDF membrane using a wet electroblotting apparatus. This transfer system requires the gel and membrane to be assembled into a sandwich that is surrounded on each side by first a layer of blotting paper, then a fiber pad and finally a plastic support grid. First, the PVDF membrane is activated by submerging it into methanol for 45 seconds, then rinsing it in milliQ water for 2 minutes before finally soaking it in transfer buffer (Tab. 23) to equilibrate the membrane.

Table 23: Transfer buffer.

Reagent	MW	1 L	[Final]
MilliQ		700 mL	
Tris	121.14	58.15 g	480 mM
Glycine	75.07	29.27 g	390 mM
QS with milliQ to:		1 L	

The blotting paper and fiber pads were likewise submerged in transfer buffer. Then the gel was removed from the tank, the wells were cut off and then the gel was also submerged in transfer buffer. To start building the sandwich, the support grid closest to the cathode was laid down first. Next, a fiber pad was placed on top of the grid and the air bubbles were rolled out. The filter paper was added in the same manner on top of the pad. The following components of the sandwich were added subsequently: the gel, membrane, paper, pad and support grid placed near the anode. In this manner, the negatively charged proteins would transfer from the gel onto the membrane as they would be migrating towards the positively-charged anode. This sandwich was inserted into a buffer tank filled with transfer buffer and the transfer was run for 90 minutes at 90 V.

After the transfer was completed, the membrane was placed into a 50 mL conical tube with the side of the membrane containing the proteins exposed to the interior of the tube. To reduce non-specific binding of the antibodies, the membrane was blocked for 1 hour at room temperature in PBS-T (Tab. 24) containing 5% milk. The membrane was then stored overnight at 4℃, without allowing the membrane to dry out. The next day the milk was poured out and replaced with 5 mL of fresh milk containing 5 µL of the 6x His mouse monoclonal antibody. The tube was then placed on the lambada rotator for 1 hour. Next, the milk was discarded and the membrane was quickly rinsed with PBS-T to remove excess antibody. Then the membrane was washed on the rotator for 15 minutes with 20 mL of PBS-T. The PBS-T was discarded and the membrane was washed twice more with PBS-T for 5 minutes. Then a secondary anti-mouse goat antibody conjugated to horse radish peroxidase (HRP) was applied to amplify the signal. 5 mL of PBS-T containing 5% milk and 5 µL of the secondary antibody was incubated with the membrane for 1 hour on the rotator. Again, the membrane was thoroughly rinsed with PBS-T as stated above. Before visualizing the blot, the two substrates of the Clarity ECL kit (BioRad) were mixed in a 1:1 ratio and then 500 µL of this ECL solution (substrate for enhanced chemiluminescence) was applied to a membrane.

After the excess ECL was removed from the membrane, the the ImageLab software on the Chemidoc was used to take a multichannel image of the membrane.

Table 24: PBS-T buffer.

Reagent	MW	5 L	[Final]
10x PBS		500 ml	1x
Tween 20	1227.72	2.5 ml	0.05%

4. Results

4.1. Generation of BF Lister 427 MiTaT 1.2 SCoAS β RNAi cell line

The TbSCoAS p2T7-Phleo plasmid (Fig. 3), which was used for the knockdown of the SCoAS β subunit via RNAi, was previously cloned by a member of the laboratory. This plasmid contained a head-to-head T7 promoter that recruited the heterologous T7 RNA polymerase to transcribe a double-stranded RNA (dsRNA) of the inserted SCoAS β coding sequence. This process was regulated by tetracycline repressor (TetR) operon sequences located just downstream of the T7 promoters. These recruited the ectopic TetR proteins, which inhibited the processivity of the T7 RNA polymerase. The addition of tetracycline in the media served to induce the RNAi by binding to the TetR and causing a conformational change that released the TetR from the DNA. The linearized plasmid was integrated into the parasite genome by homologous recombination at the minichromosome 177 repeat region. The minichromosomes in general are transcriptionally silent, thus limiting any leaky expression of the SCoAS β dsRNA from endogenous RNA polymerases. Finally, the plasmid contained the coding sequence for the phleomycin resistance protein that would confirm positive selection of parasites that integrated the plasmid. The transcription of this gene was driven by the well-defined and robust *T. brucei* rDNA promoter.

Unfortunately, successful homologous recombination in *T. brucei* is a rather rare event; therefore, a large amount of DNA was required for the transfection. For this purpose, we followed the manufacturer's suggested protocol for the GenElute HP Midiprep Kit (Sigma), which is very similar in principle to the miniprep described in the methods. This resulted in 100 µL of 3046.5 ng/uL of isolated plasmid DNA, as measured by the Nanodrop. The 260/280 ratio was used to determine the purity of the DNA sample based on the different absorption wavelengths of DNA and several contaminants, i.e. RNA, proteins and phenol. The ratio was within the 1.8 – 2.0 range and the sample was considered sufficiently pure (Tab. 25).

Table 25: Nanodrop quantification of the DNA content and purity of the isolated TbSCoAS p2T7-phleo plasmid.

Plasmid	Concentration	260/280
TbSCoASp2T7-phleo	3046.5 ng/µL	1.86

Integration into the minichromosomal locus in the trypanosomal genome was enhanced by linearizing the plasmid DNA with the Not1 enzyme, which recognizes an engineered restriction site in the middle of a 500 nt repeat region of the minichromosome. 20 μg of plasmid DNA was digested with 5 μL of Not1 for 2 hours at 37℃ to ensure the complete linearization of the plasmid (Methods, Tab. 4). The digested DNA was precipitated and then resuspended in sterile milliQ. The concentration and purity were determined using the Nanodrop (Tab. 26) and resolved on an agarose gel (Fig. 8). Importantly, the 3 observed bands (coiled, supercoiled, nicked) of the uncut plasmid are not detected in the linearized sample (expected size of 5871 nt), indicating that the digestion was complete.

Table 26: Nanodrop quantification of the DNA content and purity of the linearized TbSCoASp2T7-phleo plasmid.

Plasmid	**Concentration**	**260/280**
TbSCoASp2T7-phleo	747.4 ng/μl	1.85

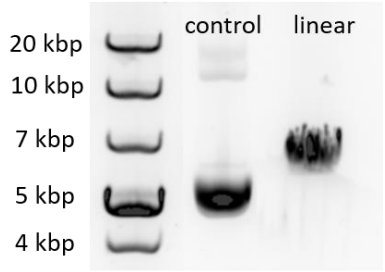

Figure 8: Not1 linearized TbSCoAS p2T7 plasmid used for T. brucei transfection. The sample was resolved on a 0.8% agarose gel and the 1 kb Plus DNA Ladder was used as a size standard. The isolated uncut plasmid was used as a control, while the plasmid digested with Not1 for 2 hours appears as a linear molecule at the expected size.

BF Lister 427 MiTat 1.2 cells grown in mid-log phase were then transfected with 12 μg of linearized SCoAS β RNAi plasmid DNA. The transfected cells were serially diluted into 24 well plates in an attempt to isolate cultures obtained from a small population of parasites that are hopefully genetically similar. After a 16 hour recovery period, the cells were then selected with 2.5 μg/mL phleomycin and the wells were monitored closely over the next two weeks. Selected clonal cell lines were then expanded and frozen in LN_2 for long-term storage. A few of the cell lines were kept in culture to analyze if SCoAS β was essential.

4.2. SCoAS β RNAi growth curves

If the BF parasite requires substrate level phosphorylation to generate mitochondrial ATP that can then be hydrolyzed by ATPase in order to maintain membrane potential, then the depletion of this enzyme should be lethal to the cells. Therefore, we compared the growth rate of uninduced cells to those induced for RNAi with the addition of tetracycline. The cell density was measured daily and the cells were split to maintain the culture in mid-log growth. The cumulative density was calculated as if the cells were allowed to proliferate indefinitely (Fig. 9, 10 & 11). The curves do not show signs of a significantly slowing growth rate compared to the control noninduced cells, which indicates that the trypanosomes were not significantly affected by the RNAi of SCoAS β.

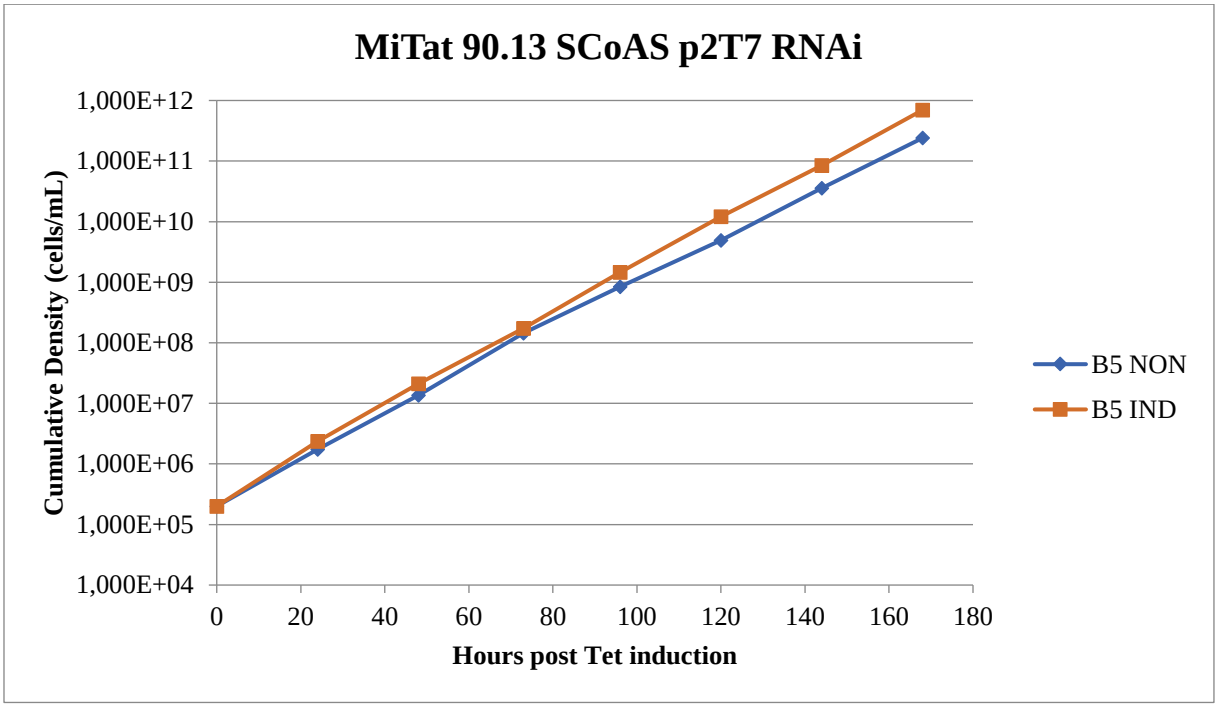

Figure 9: Growth curves of clones B5 of transfected bloodstream from BF Lister 427 MiTat 90.13 *T. brucei* cells used for RNAi knockdown of the SCoAS β subunit. The cumulative cell density was measured for cultures that were either noninduced (NON) or induced for RNAi (IND) with 1 μg/ mL tetracycline.

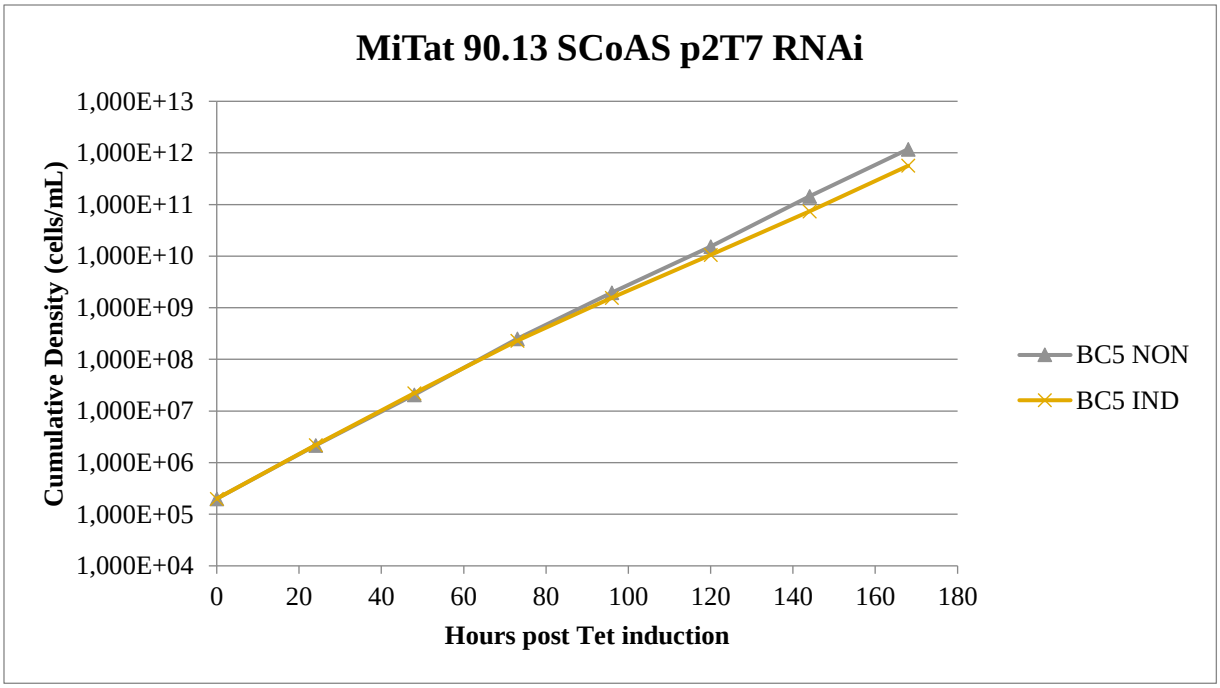

Figure 10: Growth curves of clones BC5 of transfected bloodstream from BF Lister 427 MiTat 90.13 *T. brucei* cells used for RNAi knockdown of the SCoAS β subunit. The cumulative cell density was measured for cultures that were either noninduced (NON) or induced for RNAi (IND) with 1 μg/ mL tetracycline.

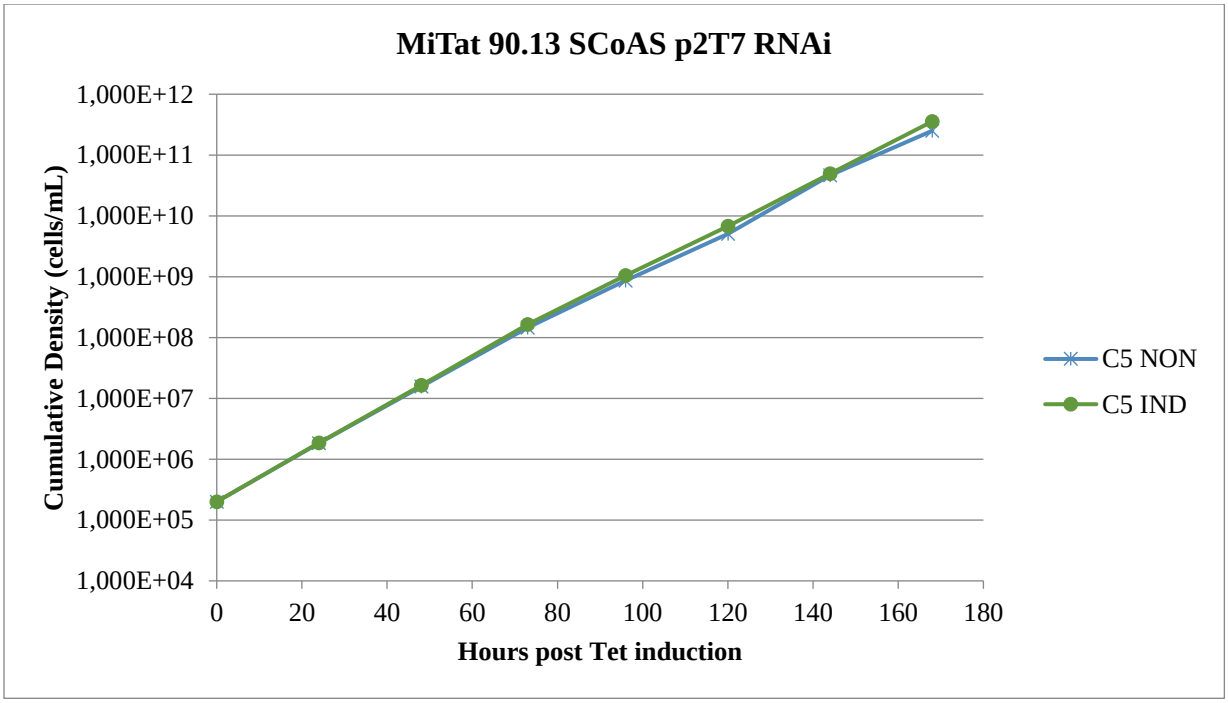

Figure 11: Growth curves of clones C5 of transfected bloodstream from BF Lister 427 MiTat 90.13 *T. brucei* cells used for RNAi knockdown of the SCoAS β subunit. The cumulative cell density was measured for cultures that were either noninduced (NON) or induced for RNAi (IND) with 1 μg/ mL tetracycline.

4.3. qPCR verification of SCoAS β RNAi

The lack of a growth phenotype in the RNAi induced cells could indicate that 1) SCoAS β is not essential in BF cells or 2) the RNAi depletion of SCoAS β was not sufficient. Therefore, it was also necessary to quantify the efficiency of the RNAi by qPCR.

We selected clone B5 to be analyzed by qPCR. It was induced with tetracycline and total RNA was extracted on days 0, 2 and 4 post induction. We chose these timepoints because the depletion of a target transcript is typically detected by day 2 in *T. brucei* RNAi cell lines. Since a growth phenotype was not detected, we also chose day 4 to harvest RNA in case the RNAi was inefficient or had a late effect. cDNA was generated and used in a relative qPCR reaction analyzed on the LightCycler 480 (Roche). The data was extracted and manipulated using the Pfaffl calculations listed previously in the Methods (Eq. 4). Using the ribosomal 18S housekeeping gene as an internal control with steady RNA expression levels, the fold change of the SCoAS β transcript at 2 and 4 days post-RNAi induction were compared to the levels of SCoAS β in the noninduced RNAi cells (Fig. 12). The results were graphed so that no change in the SCoAS β transcript would be depicted as 1.0, while any decrease in the targeted mRNA during RNAi would result in a value less than 1.0. The qPCR analysis demonstrates that the SCoAS β transcript was significantly depleted already after two days of RNAi induction. While the RNAi efficiency appears less after four days of RNAi, the transcript is still being silenced.

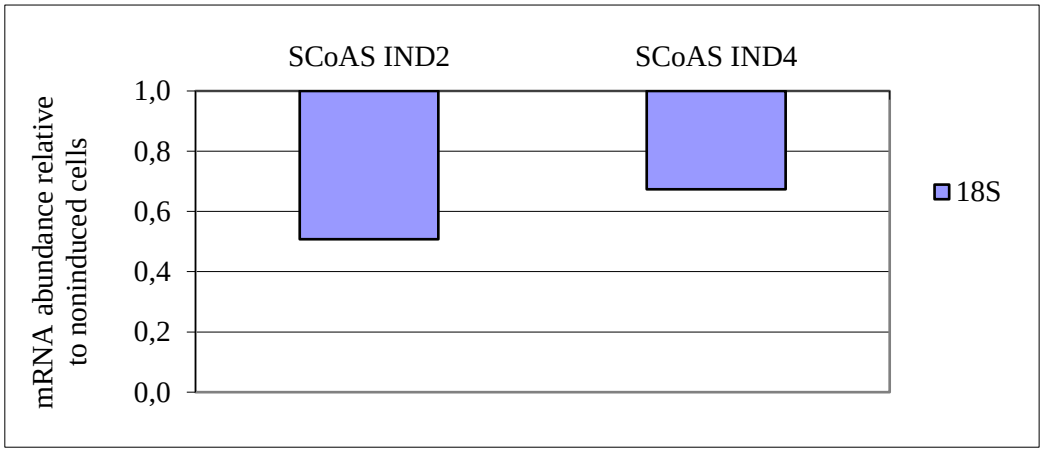

Figure 12: Results of the Pfaffl method for the relative quantification of real-time qPCR. The SCoAS mRNA values were normalized to 18S mRNA levels and then used to calculate the fold change of the target transcript on day 2 (SCoAS IND2) and day 4 (SCoAS IND4) post RNAi induction compared to SCoAS β levels measured in RNAi noninduced cells.

4.4. SCoAS β bacterial expression

The qPCR analysis determined that the RNAi effectively depleted the SCoAS β mRNA, but it does not directly address how much of the protein is still present in the parasite. This is especially true in *T. brucei,* where almost all protein expression levels are regulated post-transcriptionally. Therefore, we decided to generate a polyclonal antibody that would detect SCoAS β on western blots. This process involves expressing the *T. brucei* SCoAS β in bacterial protein expression cell lines. Then the antigen is purified from the bacterial proteins using affinity chromatography.

To induce the bacteria to express *T. brucei* SCoAS β, the coding sequence was cloned into the bacterial expression plasmid pSKB3 in a manner that fused an N-terminal 6x histidine tag to the protein so its expression can be monitored with an anti-His antibody. Chemically competent C41 *E. coli* cells were then transformed with the plasmid DNA by heat shocking the cells. Positive bacterial clones were then selected on LB agar plates containing kanamycin. To determine if the levels of inducible bacterial heterologous protein expression varied between bacterial clones, three individual cultures arising from a single clone were induced with IPTG and then harvested either before the IPTG induction or 1, 2 and 3 hours after the addition of IPTG. Whole cell lysates were prepared for SDS-PAGE and the relative amount of protein was determined by western blot analysis (Fig. 13).

Indeed, an increase in the amount of protein over time is clearly visible. Importantly, there is no detected SCoAS expression in the uninduced samples. This indicates that the inducible expression in the bacteria is tightly regulated, which can become very important if the heterologous expression is toxic for the bacteria. SCoAS protein expression is already detected at 1 hour post induction, with increasing levels of protein detected at each time point. There seems to be no significant difference in the amount of protein expression between the bacterial clones, so we chose clone 2 for future analyses. Finally, it is important to note that there is negligible protein degradation in the protein samples as the predominant band is detected at the predicted size of 48 kDa.

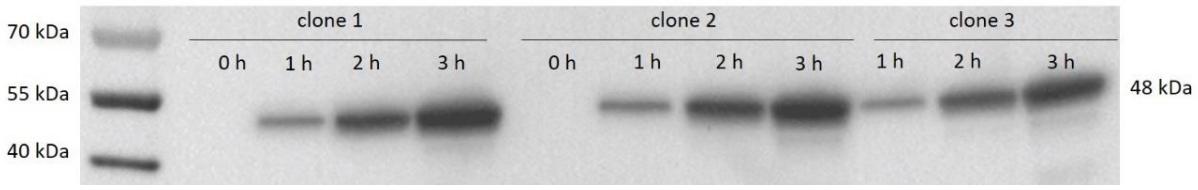

Figure 13: Western blot analysis of bacterial whole cell lysates prepared at various time points during C41 bacterial protein expression of the *T. brucei* SCoAS β. Samples were run on a precast 4-12% polyacrylamide gel. The PageRuler Prestained Protein Ladder was used as protein size standards. The SCoAS β (expected size of 48 kDa) was visualized with an anti-histidine monoclonal antibody and a secondary goat anti-mouse antibody conjugated with HRP.

4.5. SCoAS β antigen solubility

The preparation of the bacterial sample for the affinity chromatography purification process largely depends on the solubility of the expressed protein. Therefore, we tested if the expressed SCoAS β could be isolated from the soluble or insoluble fraction of the lysed bacteria.

The bacterial culture was again induced with IPTG and samples were harvested at the following time points: before induction (0 hours) and 1 & 2 hours post induction. The bacterial pellet was then lysed with lysozyme and treated with DNase to reduce the viscosity of the sample due to the release of the nuclear DNA. Following the lysis treatment, the sample was spun to pellet any insoluble material. Samples from the soluble supernatant and insoluble pellet were compared to the whole cell lysates, all of which were resolved by SDS-PAGE. The gel was then stained with Coomassie to visualize the entire protein composition of each fraction (Fig. 14). Equal percentages of total volumes were loaded for each sample to determine whether the bacterially expressed SCoAS β is predominantly soluble or not.

The protein profile is much more complex in the soluble fraction, which makes it easier to identify the likely band representing SCoAS around 48 kDa in the insoluble fraction. This becomes especially obvious in the 2 hour sample. Therefore, it would appear that SCoAS is not soluble under these conditions. The rapid expression of a heterologous protein often results in the bacteria packing the protein into insoluble inclusion bodies. It is also important to note that the wavy band detected at the bottom of the insoluble samples is most likely due to the precipitation of the high concentration of Mg^{2+}, Ca^{2+} and Cl^{-} ions added for the DNase treatment. The high salt concentration in these samples distorts the electrophoretic field and produces these artifacts, which can also distort the true migration rate of the proteins. This

explains why the observed SCoAS β protein band appears to run a little higher than the 50 kDa band in the protein ladder.

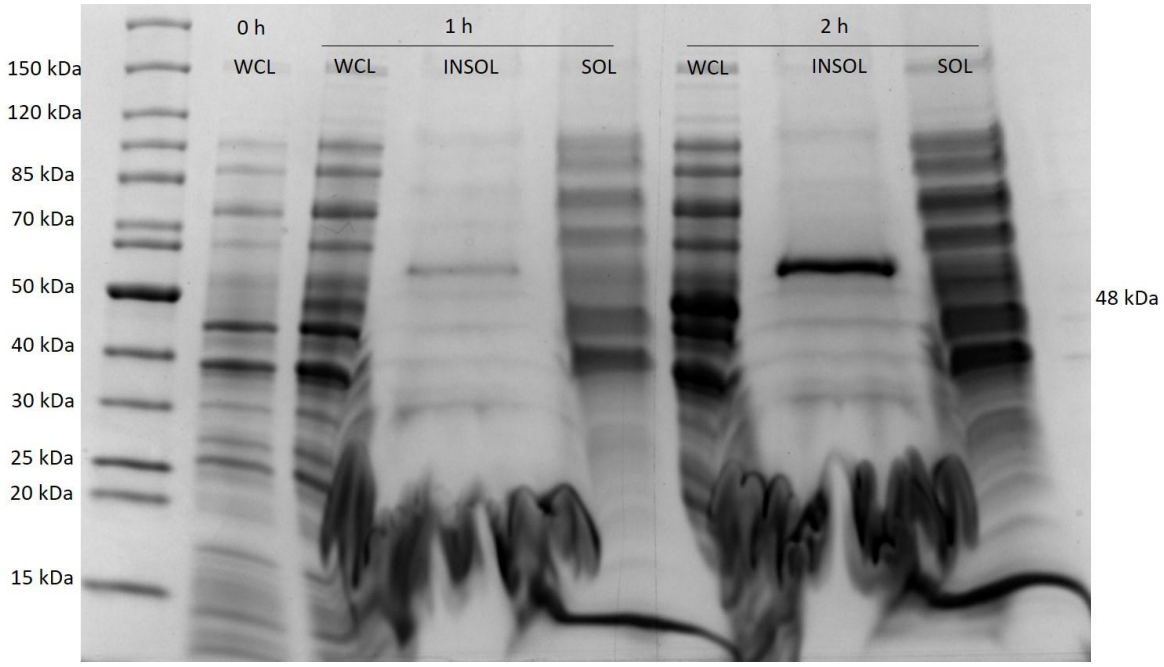

Figure 14: Coomassie stained SDS-PAGE gel of resolved proteins isolated from SCoAS β bacterial clone 2. Whole cell lysates (WCL) were compared to the insoluble (INSOL) and soluble (SOL) material produced from bacteria lysed with lysozyme. The samples were run on a precast 4-12% polyacrylamide gel, with the PageRuler Unstained Protein Ladder loaded as a size standard.

To verify that the band found in the Coomassie stained gel is indeed *T. brucei* SCoAS β, the same protein samples were analyzed by a western blot analysis. The 6x His tagged SCoAS β was visualized by probing the membrane with a primary mouse antibody that recognizes the histidine epitope (Fig. 15). The blot confirmed the previous result that the protein is present in the insoluble pellet fraction after performing the lysozyme solubility assay. Importantly, the additional manipulation of the bacterial cells didn't lead to any protein degradation of SCoAS β. The size difference between the signal detected in the WCL and the insoluble samples is again likely due to the altered migration rate of the protein sample with high concentrations of salt.

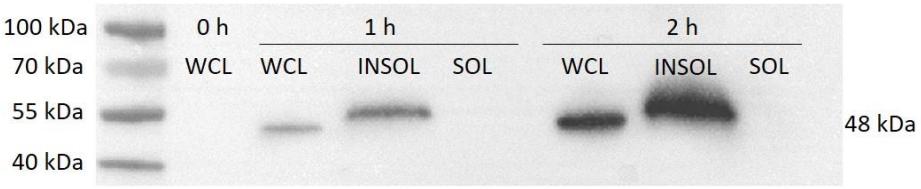

Figure 15: Western blot analysis of resolved proteins isolated from SCoAS β bacterial clone 2. Whole cell lysates (WCL) were compared to the insoluble (INSOL) and soluble (SOL) material produced from bacteria lysed with lysozyme. The samples were run on a precast 4-12% polyacrylamide gel, with the PageRuler Prestained Protein Ladder loaded as a size standard.

5. Discussion

The main aim of this thesis was to determine if SCoAS contributes to the mitochondrial ATP pool production through substrate-level phosphorylation. *Zhang et al*, published in 2010 that they observed a significant growth phenotype when SCoAS β was depleted by RNAi. The effect was so severe that after only 20 hours of induced RNAi, the cell abundance plummeted. These results were a strong indication that while the BF mitochondrion consumes ATP in this life stage, substrate phosphorylation is capable of generating ATP in the organelle to potentially offset the energetic costs of ATP hydrolysis by the ATPase. To determine the ability of the RNAi cell line to deplete the specific transcript, *Zhang et al* used a northern blot analysis to demonstrate that the SCoAS β mRNA was almost undetectable after 18 hrs. This indicates that the expected transcript was significantly depleted before the growth phenotype was observed. Since our SCoAS β knockdown in the BF Lister 427 MiTat 1.2 90-13 cell line generated no significant growth phenotype, we will explore the various reasons that could explain this discrepancy.

The very rapid onset of a lethal growth phenotype by *Zhang et al* is striking since most RNAi cell lines do not display an effect until after 48 hours of RNAi. Indeed, this is all dependent on the efficiency of the RNAi silencing and the half-life of the targeted gene product and the protein complex it is associated with. However, it is possible that the intended RNAi silencing of the target sequence produced off-target effects that could manifest in a phenotype unrelated to the depletion of just SCoAS β. These manifestations may include cell toxicity, which result independently of the RNAi of the target sequence (Fedorov, 2006). There are several ways that small interfering RNAs, siRNA, molecules can have an off-target effect (Jackson, 2010). The siRNA can target the coding region of another gene transcript with a similar sequence, which along with the on-target silencing could lead to multigene-silencing (Rual, 2007). Furthermore, it was found that siRNA may bind to the 3‘ untranslated regions of endogenous messenger RNA, mRNA, with only partial complementarity and thus regulate the transcription of the mRNA similarly to micro RNAs (Jackson, 2010). According to *Fedorov et al*, about 30% of the observed phenotypes observed with siRNA are actually caused by off-target effects. These effects can be significantly reduced by chemical modification, i.e. the addition of a 2’-*O*-methyl ribosyl substitution was found to be very effective (Fedorov, 2006). However, these statements regarding off-target effects refer to the abundant literature of siRNAs used in mammalians cells. This RNAi method is very different from what is used in trypanosomes, where 400-600 bp long dsRNA molecules are transcribed

and degraded into siRNAs. The use of such a long dsRNA to trigger RNAi in mammalian cells would be ineffective as it would only serve to induce the interferon innate immune response. On the other hand, off-target effects are relevant for all organisms and their outcome such as cell toxicity should be taken into consideration.

Fortunately, there are several methods that can be implemented to detect the presence of an off-target effect. In the case that the sequence used in the knockdown is known, we could simply choose another region of the transcript to target, since it would be unlikely that two different dsRNA molecules would create silimarly lethal off-target effects. A second approach consists of introducing a re-coded copy of the gene whose expression can be regulated – turned on and off. To ensure that this ectopic gene is not targeted by the RNAi molecules, the wobble position of every codon would be changed so it would encode the same amino acid, but the entirety of the transcript would be significantly different at the nucleotide level. Therefore, the inducible protein expression of this re-coded gene should alleviate the growth phenotype if it was due to the depletion of just the RNAi targeted gene product. If the growth phenotype would persist, it would be strong evidence of an off-target effect.

Over the years, several field isolates have been propagated in various research laboratories all over the world. The strains were initially identified by the uniform and densely packed VSG gene product expressed on the surface. Most of the seminary studies on the parasite were performed with a strain labeled BF 427 Lister MiTat 2.1. However, since the strains have been passed through several generations of labs, many are no longer absolutey sure which VSG their strain expresses. Therefore, the cell line is simply referred to as BF 427 Lister in the literature. Furthermore, while it was convenient to at first define field isolates by their VSG, this may not accurately capture the metabolic variances that can be observed across labs. Depending on how the cells are cultivated, their malleable metabolism can become more rigid, preferring specific metabolic substrates and pathways over others. Over long periods of isolated cultivation in various labs, these strains can display different energetic phenotypes from each other. This was apparent during the comparison of data from *Zíková et al, 2009* and *Coustou et al* where the RNAi of an F_1-ATP synthase subunit was performed. In the case of *Zíková et al, 2009* the knockdown already inhibited the growth of the PF Lister 427 29.13 strain in the presence of a glucose-rich medium, whereas *Coustou et al's* RNAi in PF EATRO1125 produced a growth phenotype only when glucose was removed from the medium.

While the *Zhang et al* paper did not explicitly define the *T. brucei* strain used to generate the SCoAS β RNAi cell line, they did mention that other experiments from the manuscript utilized BF 427 Lister MiTat 2.1 parasites. Since we do not know the VSG expressed on our BF 427 Lister cell line, we procured a BF 427 Lister MiTat 2.1 90-13 cell line from a collaborator. However, our results of SCoAS β RNAi in the BF Lister 427 MiTat 2.1 90-13 cell line confirmed the same negative result we observed in our lab strain (data not shown, results from a colleague). Since the exact SCoAS β RNAi sequence was not defined in *Zhang et al*, it is possible that we targeted a different region of the coding sequence than they selected and their RNAi was more effective at depleting SCoAS β levels.

T. brucei metabolic pathways depend heavily on the cells' environment, i.e. the presence of various nutrients. This is exemplified by the drastic metabolic and structural remodeling observed in the mitochondrion of the parasite as it transitions between the tsetse fly and the bloodstream of a mammalian host. Therefore, the type of media and the nutrient content should be considered. The HMI-11 medium that was used for the growth of our cell cultures is only semi-defined, as it contains 10% FBS. The nutrient content of the fetal bovine serum varies from animal to animal and therefore, the exact amount of nutrients in the medium varies slightly from batch to batch. Furthermore, *Creek et al*, demonstrate that HMI-11 contains more energy sources, amino acids and vitamins than physiologically relevant. Consequently, the *in vitro* culture might become dependent or utilize metabolites that are either not abundant or are at significantly reduced quantities in the mammalian blood. Thus, the cultured parasites no longer necessarily reflect the metabolism present in the natural parasites. In *Creek et al's* paper, a new medium, Creek's minimal medium (CMM) was developed to provide an environment better mimicking the one *in vivo,* i.e. without the large excess of nutrients. In particular, compared to HMI-11, CMM contains reduced amounts of the amino acids glutamine and cysteine, in addition to the 2.5 times less glucose. The significance of the nutrients provided to a *T. brucei* cell line used to study metabolism is best exemplified when another member of the lab observed a significant growth phenotype when the SCoAS β RNAi cell line was grown in the CMM media with minimal glucose.

Apart from this, the parasites grown *in vitro* become altered over time and lose their ability to perform certain biological processes that they would readily undergo *in vivo.* One of the most obvious differences between cells grown *in vitro* and *in vivo* is that cultures grown in the laboratory are mostly monomorphic. This means that the slender BF cannot easily differentiate into the stumpy form that is preadapted for life in the insect vector and thus

cannot complete the life cycle (Rico, 2013). Along these lines, we need to consider what additional energetic needs the parasite might encounter in a mammalian host versus a tissue flask. There has been a general consensus in the literature for the last 40 years, that the extracellular parasite in the bloodstream of the host utilizes high amounts of glucose to generate all of its ATP via glycolysis. Some of this total pool of ATP would need to be diverted to the mitochondrion where the F_oF_1-ATPase hydrolyzes ATP to maintain the essential mitochondrial membrane potential. While a parasite grown in the safe confines of a flask may not mind the loss of this ATP, BF *T. brucei* depleted of SCoAS might not have enough total cellular ATP to continuously recycle the variant surface glycoprotein (VSG) expressed on its surface when it is recognized by the host's immune system. This antigenic variation allows the parasite to prolong the infection, but it is a very energetically demanding process. There is a possibility that we don't see a growth phenotype when the cells are grown in culture, but the cellular energetic needs are much greater in the mammalian host. In fact, preliminary evidence from a colleague in the laboratory suggests that parasites completely lacking SCoAS are significantly less virulent in a mouse model.

Finally, RNAi is almost never 100% effective, meaning that there will always be some amount of the protein expressed. Therefore, we performed a qPCR to analyze the effectiveness of the knockdown. The analysis confirmed that there was a significant decrease in the SCoAS β transcript after just 48 hours of RNAi induction; however, *T. brucei* regulates its gene expression on a post-transcriptional level and thus it is hard to determine the exact amount of the enzyme subunit in the RNAi cell line from the qPCR data. Trypanosomatids, although eukaryotes, have polycistronic transcription and protein expression levels are mainly determined post-transcriptionally by RNA-binding proteins that can either stabilize or destabilize an mRNA (Clayton, 2019). When I was performing my experiments, no *T. brucei* SCoAS β antibody was available to analyze the enzyme abundance. However, a colleague in the laboratory has since performed a western blot analysis with a newly synthetized antibody generated against SCoAS β and determined that only 10-15% of the enzyme subunit is still present after 48 hours of RNAi induction. Although this result confirmed that the SCoAS was significantly depleted by RNAi, low amounts of RNA could potentially still produce a sufficient protein amount to maintain the cell's viability. Further investigations could determine whether the remaining amount of enzyme present after RNAi is enough to supress a phenotype. The only way to address this concern is to generate a cell line in which both alleles of the gene have been replaced by selectable markers. Indeed, another colleague in the

laboratory is currently characterizing this cell line to determine what the loss of this enzyme means for the parasite.

6. References

Bringaud, F., Rivière, L., Coustou, V. (2006) Energy metabolism of trypanosomatids: Adaptation to available carbon sources. *Molecular & Biochemical Parasitology* 149, 1-9.

Capewell, P., Cren-Travaillé, C., Marchesi, F., Johnston, P., Clucas, C., Benson, R.A., Gorman, T., Calvo-Alvarez, E., Crouzols, A., Jouvion, G., Jamonneau, V., Weir, W., Stevenson, M.L., O'Neill, K., Cooper, A., Kuispond Swar, N., Bucheton, B., Mumba Ngoyi, D., Garside, P., Rotureau, B., MacLeod, A. (2016) The skin is a significant but overlooked anatomical reservoir for vector-borne African trypanosomes. *eLife* 5: e17716

Clayton, C. (2019) Regulation of gene expression in trypanosomatids: living with polycistronic transcription. *Open Biology* 9:190072.

Coustou, V., Biran, M., Breton, M., Guegan, F., Rivière, L., Plazolles, N., Nolan, D., Barrett, M.P., Franconi, J-M. et Bringaud, F. (2008) Glucose-induced Remodeling of Intermediary and Energy Metabolism in Procyclic *Trypanosoma brucei. Journal of Biological Chemistry* 283, 16342-16354.

Creek, D.J., Nijagal, B., Kim, D-H., Rojas, F., Matthews, K.R. and Barrett, M.P. (2013) Metabolomics Guides Rational Development of a Simplified Cell Culture Medium for Drug Screening against *Trypanosoma brucei. Antimicrobial Agents and Chemotherapy* 57, 2768-2779.

Dyer, N.A., Rose, C., Ejeh, N.O., and Acosta-Serrano, A. (2013) Flying tryps: survival and maturation of trypanosomes in tsetse flies. *Trends in Parasitology* 29, 188-196.

Fedorov, Y., Anderson, E.M., Birmingham, A., Reynolds, A., Karpilow, J., Robinson, K., Leake, D., Marshall, W.S. and Khvorova, A. (2006) Off-target effects by siRNA can induce toxic phenotype. *RNA Journal* 12, 1188-1196.

Jackson, A.L., Linsley, R.S. (2010) Recognizing and avoiding siRNA off-target effects for target identification and therapeutic application. *Nature Reviews* 9, 57-67.

Jenkins, T.M., Eisenthal, R., and Weitzman, P.D.J. (1988) Two distinct succinate thiokinases in both bloodstream and procyclic forms of Trypanosoma brucei. *Biochemical and Biophysical Research Communications* 151, 257-261.

Mony, B.M., and Matthews, K.R. (2015) Assembling the components of the quorum sensing pathway in African trypanosomes: Quorum sensing pathway in African trypanosomes. *Molecular Microbiology* 96, 220-232

Ostergaard, E. (2008) Disorders caused by deficiency in succinate-CoA ligase. *Journal of Inherited Metabolic Disease* 31, 226-229.

Pfaffl, M.W. (2001) A new mathematical model for relative quantification in real-time RT-PCR, *Nucleic Acids Research* 29, 2001-2007.

Product Information GenElute HP Plasmid Midiprep Kit.

Product Information GenElute HP Plasmid Miniprep Kit.

Product Information LightCycler 480 SYBR Green I Master Mix.

Product Information RNeasy MinElute Cleanup Kit.

Product Information RNeasy Mini Kit.

Product Information TaqMan Reverse Transcription Kit.

Product Information TURBO DNA-free Kit.

Rico, E., Rojas, F., Mony, B.M., Szoor, B., MacGregor, P. and Matthews K.R. (2013) Bloodstream form pre-adaptation to the tsetse fly in *Trypanosoma brucei*. *Frontiers in Cellular and Infection Microbiology* 3, 78.

Rijo-Ferreira, F., Carvalho, T., Afonso, C., Sanches-Vaz, M., Costa, R.M., Figueiredo, L.M., and Takahashi, J.S. (2018) Sleeping sickness is a circadian disorder. *Nature Communications* 9:62.

Rivière, L., Moreau, P., Allmann, S., Hahn, M., Biran, M., Plazolles, N., Franconi, J., Boshart, M. and Bringaud, F., (2009) Acetate produced in the mitochondrion is the essential precursor for lipid biosynthesis in procyclic trypanosomes. *PNAS* 106, 12694-12699.

Rual, J-F., Klitgord, N. and Achaz, G. (2007) Novel insights into RNAi off-target effects using *C. elegans* paralogs. *BMC Genomics* 8:106.

Sharma, R., Gluenz, E., Peacock, L., Gibson, W., Gull, K., and Carrington, M. (2009) The heart of darkness: growth and form of Trypanosoma brucei in the tsetse fly. *Trends in Parasitology* 25, 517-524.

Silva Pereira, S., Trinidade, S., De Niz, M., Figueiredo, L.M. (2019) Tissue tropism in parasitic diseases. *Open Biology*. 9: 190036.

Smith, T.K., Bringaud, F., Nolan, D.P., and Figueiredo, L.M. Metabolic reprogramming during the Trypanosoma brucei life cycle. [version 2; referees: 4 approved] *F1000Research* 2017, **6**(F1000 Faculty Rev): 683.

van Weelden, S.W.H., van Hellemond, J.J., Opperdoes, F.R., and Tielens, A.G.M. (2005) New Functions for Parts of the Krebs Cycle in Procyclic Trypanosoma brucei, a Cycle Not Operating as a Cycle. *Journal of Biological Chemistry* 280, 12451-12460.

World Health Organization [online]. Available from WWW: https://www.who.int/news-room/fact-sheets/detail/trypanosomiasis-human-african-(sleeping-sickness) (accessed May 5th 2019).

Zhang, X., Cui, J., Nilsson, D., Gunasekera, K., Chanfon, A., Song, X., Wang, H., Xu, Y. and Ochsenreiter, T. (2010) The *Trypanosoma brucei* MitoCarta and its regulation and splicing pattern during development. *Nucleic Acid Research* 38, 7378-7387.

Zíková, A., Schnaufer, A., Dalley, R.A., Panigrahi, A.K. and Stuart, K.D. (2009) The F_oF_1-ATP Synthase Complex Novel Subunits and Is Essential for Procyclic *Trypanosoma brucei*. *PLOS Pathogens* 5: e1000436.

Zíková, A., Verner, Z., Nenarokova, A., Michels, P.A.M., Lukeš, J. (2017) A paradigm shift: The mitoproteomes of procyclic and bloodstream Trypanosoma brucei are comparably complex. *PLOS Pathogens* 13: e1006679.